Neural Dynamics of Form Perception: Boundary Completion, Illusory Figures, and Neon Color Spreading

Stephen Grossberg and Ennio Mingolla
Center for Adaptive Systems, Boston University

A real-time visual processing theory is used to analyze real and illusory contour formation, contour and brightness interactions, neon color spreading, complementary color induction, and filling-in of discounted illuminants and scotomas. The theory also physically interprets and generalizes Land's retinex theory. These phenomena are traced to adaptive processes that overcome limitations of visual uptake to synthesize informative visual representations of the external world. Two parallel contour sensitive processes interact to generate the theory's brightness, color, and form estimates. A *boundary contour* process is sensitive to orientation and amount of contrast but not to direction of contrast in scenic edges. It synthesizes boundaries sensitive to the global configuration of scenic elements. A *feature contour* process is insensitive to orientation but sensitive to both amount of contrast and to direction of contrast in scenic edges. It triggers a diffusive filling-in of featural quality within perceptual domains whose boundaries are determined by completed boundary contours. The boundary contour process is hypothesized to include cortical interactions initiated by hypercolumns in Area 17 of the visual cortex. The feature contour process is hypothesized to include cortical interactions initiated by the cytochrome oxydase staining blobs in Area 17. Relevant data from striate and prestriate visual cortex, including data that support two predictions, are reviewed. Implications for other perceptual theories and axioms of geometry are discussed.

1. Illusions as a Probe of Adaptive Visual Mechanisms

A fundamental goal of visual science is to explain how an unambiguous global visual representation is synthesized in response to ambiguous local visual cues. The difficulty of this problem is illustrated by two recurrent themes in visual perception: Human observers often do not see images that are retinally present, and they often do see images that are not retinally present. A huge data base concerning visual illusions amply illustrates the complex and often paradoxical relationship between scenic image and visual percept.

That paradoxical data abound in the field of visual perception becomes more understandable through a consideration of how visual information is acquired. For example, light passes through retinal veins before it reaches retinal photoreceptors, and light does not influence the retinal regions corresponding to the blind spot or retinal scotomas. The percepts of human observers are not distorted, however, by their retinal veins or blind spots during normal viewing conditions. Thus some images that are retinally present are not perceived because our visual processes are adaptively designed to free our percepts from imperfections of the visual uptake process. The same adaptive mechanisms that can free our percepts from images of retinal veins can also generate paradoxical percepts, as during the perception of stabilized images (Krauskopf, 1963; Pritchard, 1961; Pritchard, Heron, & Hebb, 1960; Riggs, Ratliff, Cornsweet, & Cornsweet, 1953; Yarbus, 1967). The same adaptive mechanisms that can compensate for the blind spot and certain scotomas can also generate paradoxical percepts, as during

filling-in reactions of one sort or another (Arend. Buehler. & Lockhead. 1971; Gellatly, 1980: Gerrits. de Haan, & Vendrick, 1966; Gerrits & Timmerman, 1969; Gerrits & Vendrick, 1970; Kanizsa, 1974; Kennedy, 1978, 1979. 1981: Redies & Spillmann, 1981; Van Tuijl. 1975; Van Tuijl & de Weert, 1979; Van Tuijl & Leeuwenberg, 1979; Yarbus, 1967).

These examples illustrate the general theme that many paradoxical percepts may be expressions of adaptive brain designs aimed at achieving informative visual representations of the external world. For this reason, paradoxical percepts may be used as probes and tests of the mechanisms that are hypothesized to instantiate these adaptive brain designs. The present article makes particular use of data about illusory figures (Gellatly, 1980; Kanizsa, 1974; Kennedy, 1978, 1979, 1981; Parks, 1980; Parks & Marks, 1983; Petry, Harbeck, Conway, & Levey, 1983) and about neon color spreading (Redies & Spillmann, 1981: Van Tuijl. 1975: Van Tuijl & de Weert, 1979: Van Tuijl & Leeuwenberg, 1979) to refine the adaptive designs and mechanisms of a real-time visual processing theory that is aimed at predicting and explaining data about depth. brightness, color. and form perception (Carpenter & Grossberg, 1981, 1983; Cohen & Grossberg, 1983. 1984, in press; Grossberg, 1981. 1983a. 1983b, 1984a; Grossberg & Cohen, 1984; Mingolla & Grossberg, 1984).

As in every theory about adaptive behavior, it is necessary to specify precisely the sense in which its targeted data are adaptive without falling into logically circular arguments. In the present work, this specification takes the form of a new perceptual processing principle, which we call the *boundary–feature trade-off*. The need for such a principle can begin to be seen by considering how the perceptual system can generate behaviorally effective internal representations that compensate for several imperfections of the retinal image.

2. From Noisy Retina to Coherent Percept

Suppressing the percept of stabilized retinal veins is far from sufficient to generate a usable percept. The veins may occlude and segment scenic images in several places. Even a single scenic edge can be broken into several disjoint components. Somehow in the final percept, broken retinal edges are completed and occluded retinal color and brightness signals are filled-in. These completed and filled-in percepts are, in a strict mechanistic sense, illusory percepts.

Observers are often not aware of which parts of a perceived edge are "real" and which are "illusory." This fact clarifies why data about illusory figures are so important for discovering the mechanisms of form perception. This fact also points to one of the most fascinating properties of visual percepts. Although many percepts are, in a strict mechanistic sense, "illusory" percepts, they are often much more veridical, or "real," than the retinal data from which they are synthesized. This observation clarifies a sense in which each of the antipodal philosophical positions of realism and idealism is both correct and incorrect, as is often the case with deep but partial insights.

The example of the retinal veins suggests that two types of perceptual process, boundary completion and featural filling-in, work together to synthesize a final percept. In such a vague form, this distinction generates little conceptual momentum with which to build a theory. Data about the perception of artificially stabilized images provide further clues. The classical experiments of Krauskopf (1963) and Yarbus (1967) show that if certain scenic edges are artificially stabilized with respect to the retina, then colors and brightnesses that were previously bounded by these edges are seen to flow across, or fill-in, the percept until they are contained by the next scenic boundary. Such data suggest that the processes of boundary completion and featural filling-in can be dissociated.

The boundary–feature trade-off makes precise the sense in which either of these processes, by itself, is insufficient to generate a final percept. Boundary–feature trade-off also suggests that the rules governing either process can only be discovered by studying how the two processes interact. This is true because each system is designed to offset insufficiencies of the other system. In particular, the process of boundary completion, by itself, could at best generate a world of outlines or cartoons. The process of featural filling-in, by itself, could at best generate a world of formless brightness and color qualities.

Our theory goes further to suggest the more radical conclusion that the process of boundary completion, by itself, would generate a world of invisible outlines, and the process of featural filling-in, by itself, would generate a world of invisible featural qualities.

This conclusion follows from the realization that an early stage of both boundary processing and of feature processing consists of the extraction of different types of contour information. These two contour-extracting processes take place in parallel, before their results are reintegrated at a later processing stage. Previous perceptual theories have not clearly separated these two contour-extracting systems. One reason for this omission is that, although each scenic edge can activate both the boundary contour system and the feature contour system, only the net effect of their interaction at a later stage is perceived. Another reason is that the completed boundaries, by themselves, are not visible. They gain visibility by restricting featural filling-in and thereby causing featural contrast differences across the perceptual space. The ecological basis for these conclusions becomes clearer by considering data about stabilized images (Yarbus, 1967) alongside data about brightness and color perception (Land, 1977). These latter data can be approached by considering another ambiguity in the optical input to the retina.

The visual world is typically viewed in inhomogeneous lighting conditions. The scenic luminances that reach the retina thus confound variable lighting conditions with invariant object colors. It has long been known that the brain somehow "discounts the illuminant" in order to generate percepts whose colors are more veridical than those in the retinal image (Helmholtz, 1962). The studies of Land (1977) have refined this insight by showing that the perceived colors within a picture constructed from overlapping patches of color are determined by the relative contrasts at the edges between successive patches. Lighting conditions can differ considerably as one moves across each colored patch. At each patch boundary, lighting conditions typically change very little. A measure of relative featural contrast across such a boundary therefore provides a good local estimate of object reflectances.

Land's results about discounting the illuminant suggest that an early stage of the featural extraction process consists in computing featural contrasts at scenic edges. Data such as that of Yarbus (1967), which show that boundaries and features can be dissociated, then suggest that the extraction of feature contour and boundary contour information are two separate processes.

The Land (1977) data also support the concept of a featural filling-in process. Discounting the illuminant amounts to suppressing the color signals from within the color patches. All that remains are nondiscounted feature contrasts at the patch boundaries. Without featural filling-in, we would perceive a world of colored edges, instead of a world of extended forms. The present theory provides a physical interpretation and generalization of the Land retinex theory of brightness and color perception (Grossberg, 1984a), including an explanation of how we can see extended color domains. This explanation is summarized in Section 18.

Our theory can be understood entirely as a perceptual processing theory. As its perceptual constructs developed, however, they began to exhibit striking formal similarities with recent neural data. Some of these neural analogs are summarized in Table 1 below. Moreover, two of the theory's predictions about the process of boundary completion have recently received experimental support from recordings by von der Heydt, Peterhans, and Baumgartner (1984) on cells in Area 18 of the monkey visual cortex. Neurophysiological linkages and predictions of the theory are more completely described in Section 20. Due to the existence of this neural interpretation, the formal nodes in the model network are called *cells* throughout the article.

3. Boundary Contour System and Feature Contour System

Our theory claims that two distinct types of edge, or contour, computations are carried out within parallel systems during brightness, color, and form perception (Grossberg, 1983a, 1983b, 1984a). These systems are called the *boundary contour system* (BCS) and the *feature contour system* (FCS). Boundary contour signals are used to generate perceptual

boundaries, both "real" and "illusory." Feature contour signals trigger the filling-in processes whereby brightnesses and colors spread until they either hit their first boundary contours or are attenuated due to their spatial spread. Boundary contours are not, in isolation, visible. They gain visibility by restricting the filling-in that is triggered by feature contour signals and thereby causing featural contrasts across perceptual space.

These two systems obey different rules. We will summarize the main rules before using them to explain paradoxical visual data. Then we will explain how these rules can be understood as consequences of boundary–feature trade-off.

4. Boundary Contours and Boundary Completion

The process whereby boundary contours are built up is initiated by the activation of oriented masks, or elongated receptive fields, at each position of perceptual space (Hubel & Wiesel, 1977). An oriented mask is a cell, or cell population, that is selectively responsive to scenic edges. Each mask is sensitive to scenic edges that activate a prescribed small region of the retina, if the edge orientations lie within a prescribed band of orientations with respect to the retina. A family of such oriented masks exists at every network position, such that each mask is sensitive to a different band of edge orientations within its prescribed small region of the scene.

Orientation and Contrast

The output signals from the oriented masks are sensitive to the *orientation* and to the *amount* of contrast, but not to the *direction* of contrast, at an edge of a visual scene. A vertical boundary contour can thus be activated by either a close-to-vertical dark–light edge or a close-to-vertical light–dark edge at a fixed scenic position. The process whereby two like-oriented masks that are sensitive to direction of contrast at the same perceptual location give rise to an output signal that is not sensitive to direction of contrast is designated by a plus sign in Figure 1a.

Short-Range Competition

The outputs from these masks activate two successive stages of short-range competition that obey different rules of interaction.

1. The cells that react to output signals due to like-oriented masks compete between nearby perceptual locations (Figure 1b). Thus, a mask of fixed orientation excites the like-oriented cells at its location and inhibits the like-oriented cells at nearby locations. In other words, an on-center off-surround organization of like-oriented cell interactions exists around each perceptual location. It may be that these spatial interactions form part of the network whereby the masks acquire their orientational specificity during development. This possibility is not considered in this article.

2. The outputs from this competitive stage input to the next competitive stage. Here, cells compete that represent perpendicular orientations at the same perceptual location (Figure 1c). This competition defines a push–pull opponent process. If a given orientation
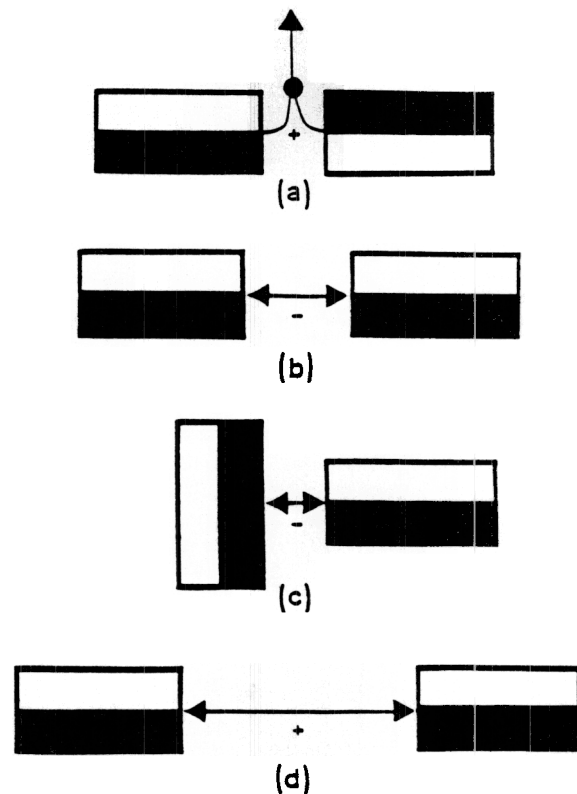

Figure 1. (a) Boundary contour signals sensitive to the orientation and amount of contrast at a scenic edge, but not to its direction of contrast. (b) Like orientations compete at nearby perceptual locations. (c) Different orientations compete at each perceptual location. (d) Once activated, aligned orientations can cooperate across a larger visual domain to form "real" and "illusory" contours.

is inhibited, then its perpendicular orientation is disinhibited.

In summary, a stage of competition between like orientations at different, but nearby, positions is followed by a stage of competition between perpendicular orientations at the same position.

Long-Range Oriented Cooperation and Boundary Completion

The outputs from the second competitive stage input to a spatially long-range cooperative process. We call this process the *boundary completion* process. Outputs due to like-oriented masks that are approximately aligned across perceptual space can cooperate via this process to synthesize an intervening boundary. We show how both "real" and "illusory" boundaries can be generated by this boundary completion process.

The following two demonstrations illustrate a boundary completion process with the above properties of orientation and contrast, short-range competition, and long-range cooperation and boundary completion. In Figure 2a, four black pac-man figures are arranged at the vertices of an imaginary square on a white background. The famous illusory Kanizsa (1974) square can then be seen. The same is true when two pac-man figures are black, the other two are white, and the background is gray, as in Figure 2b. The black pac-man figures form dark–light edges with respect to the gray background. The white pac-man figures form light–dark edges with respect to the gray background. The visibility of illusory edges around the illusory square shows that a process exists that is capable of completing boundaries between edges with opposite directions of contrast. The boundary completion process is thus sensitive to orientational alignment across perceptual space and to amount of contrast, but not to direction of contrast.

Another demonstration of these boundary completing properties can be constructed as follows. Divide a square into two equal rectangles along an imaginary boundary. Color one rectangle a uniform shade of gray. Color the other rectangle in shades of gray that progress from light to dark as one moves from End 1 of the rectangle to End 2 of the rectangle. Color End 1 a lighter shade than

the uniform gray of the other rectangle, and color End 2 a darker shade than the uniform gray of the other rectangle. As one moves from End 1 to End 2, an intermediate gray region is passed whose luminance approximately equals that of the uniform rectangle. At End 1, a light–dark edge exists from the nonuniform rectangle to the uniform rectangle. At End 2, a dark–light edge exists
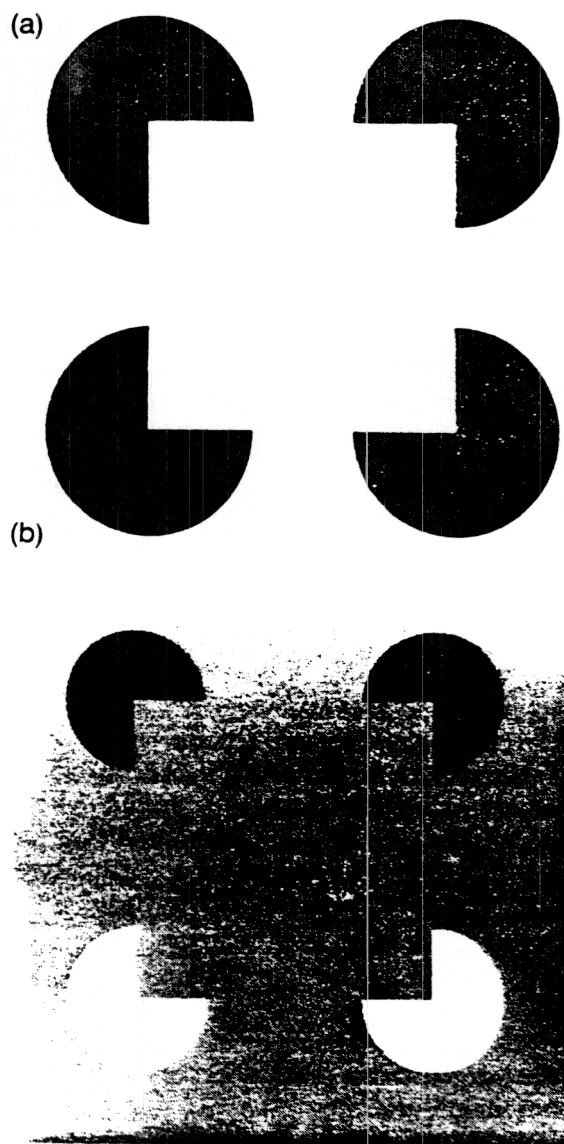

Figure 2. (a) Illusory Kanizsa square induced by four black pac-man figures. (From "Subjective Contours" by G. Kanizsa, 1976, *Scientific American, 234,* p. 51. Copyright 1976 by Scientific American, Inc. Adapted by permission.) (b) An illusory square induced by two black and two white pac-man figures on a gray background. (Illusory contours can thus join edges with opposite directions of contrast. This effect may be weakened by the photographic reproduction process.)

from the nonuniform rectangle to the uniform rectangle. An observer can see an illusory edge that joins the two edges of opposite contrast and separates the intermediate rectangle region of equal luminance.

Although this boundary completion process may seem paradoxical when its effects are seen in Kanizsa squares, we hypothesize that this process is also used to complete boundaries across retinal scotomas, across the faded images of stabilized retinal veins, and between all perceptual domains that are separated by sharp brightness or color differences.

Binocular Matching

A monocular boundary contour can be generated when a single eye views a scene. When two eyes view a scene, a binocular interaction can occur between outputs from oriented masks that respond to the same retinal positions of the two eyes. This interaction leads to binocular competition between perpendicular orientations at each position. This competition takes place at, or before, the competitive stage.

Although binocular interactions occur within the boundary contour system, they will not be needed to explain this article's targeted data.

Boundary contours are like frames without pictures. The pictorial data themselves are derived from the feature contour system. We suggest that the same visual source inputs in parallel to both the boundary contour system and the feature contour system, and that the outputs of both types of processes interact in a context-sensitive way at a later stage.

5. Feature Contours and Diffusive Filling-In

The feature contour process obeys different rules of contrast than does the boundary contour process.

Contrast

The feature contour process is insensitive to the *orientation* of contrast in a scenic edge, but it is sensitive to both the *direction* of contrast as well as to the *amount* of contrast, unlike the boundary contour process. Speak-

ing intuitively, in order to compute the relative brightness across a scenic boundary, it is necessary to keep track of which side of the scenic boundary has a larger reflectance. Sensitivity to direction of contrast is also used to determine which side of a red–green scenic boundary is red and which is green. Due to its sensitivity to the amount of contrast, feature contour signals discount the illuminant. We envisage that three parallel channels of double-opponent feature contour signals exist: light–dark, red–green, and blue–yellow (Boynton, 1975; DeValois & DeValois, 1975; Mollon & Sharpe, 1983), These double-opponent cells are replicated in multiple cellular fields that are maximally sensitive to different spatial frequencies (Graham, 1981; Graham & Nachmias, 1971). Both of these processing requirements are satisfied in a network that is called a *gated dipole field* (Grossberg, 1980, 1982). The detailed properties of double-opponent gated dipole fields are not needed in this article. Hence they are not discussed further. A variant of the gated dipole field design is, however, used to instantiate the boundary contour system in Section 15.

The feature contour process also obeys different rules of spatial interaction than those governing the boundary contour process.

Diffusive Filling-In

Boundary contours activate a boundary completion process that synthesizes the boundaries which define monocular perceptual domains. Feature contours activate a diffusive filling-in process that spreads featural qualities, such as brightness or color, across these perceptual domains. Figure 3 depicts the main properties of this filling-in process.

We assume that featural filling-in occurs within a syncytium of cell compartments. By a syncytium of cells, we mean a regular array of intimately connected cells such that contiguous cells can easily pass signals between each other's compartment membranes. A feature contour input signal to a cell of the syncytium activates that cell. Due to the syncytial coupling of this cell with its neighbors, the activity can rapidly spread to neighboring cells, then to neighbors of the neighbors, and so on. Because the spreading occurs
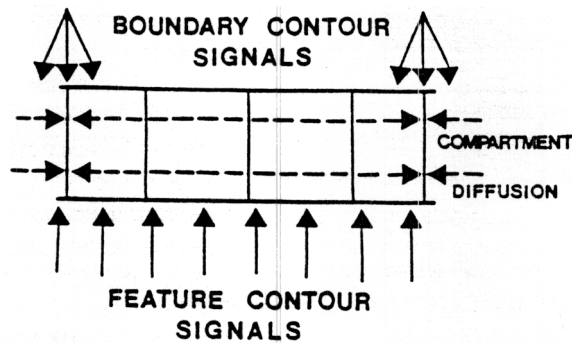
BOUNDARY CONTOUR SIGNALS

COMPARTMENT

DIFFUSION

FEATURE CONTOUR SIGNALS

Figure 3. Monocular brightness and color stage domain (MBC). (Monocular feature contour signals activate cell compartments that permit rapid lateral diffusion of activity, or potential, across their compartment boundaries, except at those compartment boundaries that receive boundary contour signals from the BCS stage of Figure 4. Consequently the feature contour signals are smoothed except at boundaries that are completed within the BCS stage.)

via a diffusion of activity (Cohen & Grossberg, in press; Grossberg, 1984a), it tends to average the activity that is triggered by a feature contour input signal across the cells that receive this spreading activity. This averaging of activity spreads across the syncytium with a space constant that depends on the electrical properties of both the cell interiors and their membranes. The electrical properties of the cell membranes can be altered by boundary contour signals in the following way.

A boundary contour signal is assumed to decrease the diffusion constant of its target cell membranes within the cell syncytium. It does so by acting as an inhibitory gating signal that causes an increase in cell membrane resistance. A boundary contour signal hereby creates a barrier to the filling-in process at its target cells.

This diffusive filling-in reaction is hypothesized to instantiate featural filling-in over retinal scotomas, over the faded images of stabilized retinal veins, and over the illuminants that are discounted by feature contour preprocessing.

Three types of spatial interaction are implied by this description of the feature contour system: (a) *Spatial frequency preprocessing*—feature contour signals arise as the outputs of several double-opponent networks whose different receptive field sizes make them maximally sensitive to different spatial frequencies.

(b) *Diffusive filling In*—feature contour signals within each spatial scale then cause activity to spread across that scale's cell syncytium. This filling-in process has its own diffusive bandwidth. (c) *Figural boundaries*—Boundary contour signals define the limits of featural filling-in. Boundary contours are sensitive to the configuration of all edges in a scene, rather than to any single receptive field size.

Previous perceptual theories have tended to focus on one or another of these factors, but not on their interactive properties.

6. Macrocircuit of Processing Stages

Figure 4 describes a macrocircuit of processing stages into which the microstages of the boundary contour system and feature contour system can be embedded. The processes described by this macrocircuit were introduced to explain how global properties of depth, brightness, and form information can be generated from monocularly and bin-
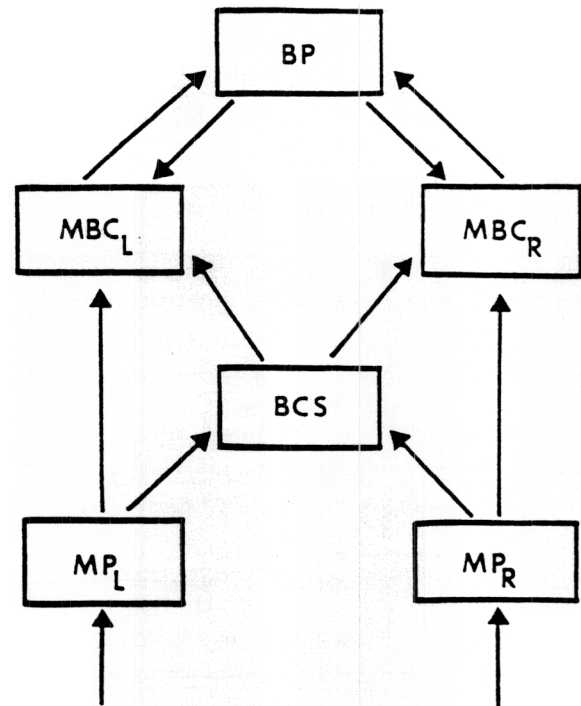

Figure 4. Macrocircuit of processing stages. (Table 1 lists the functional names of the abbreviated stages and indicates a plausible neural interpretation of these stages. Boundary contour formation is assumed to occur within the BCS stage. Its output signals to the monocular MBC_L and MBC_R stages define boundaries within which feature contour signals from MP_L and MP_R, respectively, can trigger the spreading, or diffusion, of featural quality.)

Table 1
Summary of Neural Analogs

Abbreviation	Full name	Neural interpretation
MP_L	Left monocular preprocessing stage	Lateral geniculate nucleus
MP_R	Right monocular preprocessing stage	Lateral geniculate nucleus
BCS	Boundary contour synthesis stage	Interactions initiated by the hypercolumns in striate cortex—Area 17 (Hubel & Wiesel, 1977)
MBC_L	Left monocular brightness and color stage	Interactions initiated by the cytochrome oxydase staining blobs—Area 17; (Hendrickson, Hunt, & Wu, 1981; Horton & Hubel, 1981; Hubel & Livingstone, 1981; Livingstone & Hubel, 1982)
MBC_R	Right monocular brightness and color stage	Interactions initiated by the cytochrome oxydase staining blobs—Area 17
BP	Binocular percept stage	Area V4 of the prestriate cortex (Zeki, 1983a, 1983b)

ocularly viewed patterns (Grossberg, 1983b, 1984a). Table 1 lists the full names of the abbreviated macrocircuit stages, as well as their neural interpretation.

Each monocular preprocessing (MP) stage MP_L and MP_R can generate inputs, in parallel, to its boundary contour system and its feature contour system. The pathway $MP_L \rightarrow BCS$ carries inputs to the left-monocular boundary system. The pathway $MP_L \rightarrow MBC_L$ carries inputs to the left-monocular feature contour system. Only after all the stages of scale-specific, orientation-specific, contrast-specific, competitive, and cooperative interactions take place within the BCS stage, as in Section 4, does this stage give rise to boundary contour signals $BCS \rightarrow MBC_L$ that act as barriers to the diffusive filling-in triggered by $MP_L \rightarrow MBC_L$ feature contour signals, as in Section 5. The divergence of the pathways $MP_L \rightarrow MBC_L$ and $MP_L \rightarrow BCS$ allows the boundary contour system and the feature contour system to be processed according to their different rules before their signals recombine within the cell syncytia.

7. Neon Color Spreading and Complementary Color Induction

The phenomenon of neon color spreading illustrates the existence of boundary contours and of feature contours in a vivid way. Redies and Spillmann (1981), for example, reported an experiment using a solid red cross and an Ehrenstein figure. When the solid red cross is perceived in isolation, it looks quite unin-

teresting (Figure 5a). When an Ehrenstein figure is perceived in isolation, it generates an illusory contour whose shape (e.g., circle or diamond) depends on the viewing distance. When the red cross is placed inside the Ehrenstein figure, the red color flows out of its containing contours and tends to fill the illusory figure (Figure 5b).

Our explanation of this percept uses all of the rules that we listed. We suggest that vertical boundary contours of the Ehrenstein figure inhibit contiguous boundary contours of like orientation within the red cross. This property uses the orientation and contrast sensitivity of boundary masks (Figure 1a) and their ability to inhibit like-oriented nearby cells, irrespective of direction of contrast (Figure 1a and 1b). This inhibitory action within the BCS does not prevent the processing of feature contour signals from stage MP_L to stage MBC_L and from stage MP_R to stage MBC_R, because boundary contour signals and feature contour signals are received by MBC_L and MBC_R despite the fact that some of their corresponding boundary contour signals are inhibited within the BCS stage.

The inhibition of these boundary contour signals within the BCS stage allows the red featural activity to diffuse outside of the red cross. The illusory boundary contour that is induced by the Ehrenstein figure restricts the diffusion of this red-labeled activation. Thus during neon color spreading, one can "see" the difference between boundary contours and feature contours, as well as the role of

illusory boundary contours in restricting the diffusion of featural activity. In Figure 5b, the illusory boundary induced by the Ehrenstein figure restricts the flow of red featural quality, but the "real" boundary of the cross does not. This percept illustrates that boundary contours, both "real" and "illusory," are generated by the same process.

The illusory contour in Figure 5b tends to be perpendicular to its inducing Ehrenstein figures. Thus, the Ehrenstein figure generates two simultaneous effects. It inhibits like-ori-

ented boundary contours at nearby positions, and it excites perpendicularly oriented boundary contours at the same nearby positions. We explain this effect as follows. The boundary contours of the Ehrenstein figure inhibit contiguous like-oriented boundary contours of the red cross, as in Figure 1b. By Figure 1c, perpendicular boundary contours at each perceptual position compete as part of a push–pull opponent process. By inhibiting the like-oriented boundary contours of the red cross, perpendicularly oriented boundary contours at the corresponding positions are activated due to disinhibition. These disinhibited boundary contours can then cooperate with other approximately aligned boundary contours to form an illusory contour, as in Figure 1d. This cooperative process further weakens the inhibited boundary contours of the red cross, as in Figure 1c, thereby indicating why a strong neon effect depends on the percept of the illusory figure.

Redies and Spillmann (1981) systematically varied the distance of the red cross from the Ehrenstein figure—their relative orientations, their relative sizes, and so forth—to study how the strength of the spreading effect changes with scenic parameters. They report that "thin [red] flanks running alongside the red connecting lines" (Redies & Spillmann, 1981, p. 679) can occur if the Ehrenstein figure is slightly separated from the cross or if the orientations of the cross and the Ehrenstein figure differ. In our theory, the orientation specificity (Figure 1a) and distance dependence (Figure 1b) of the inhibitory process among like-oriented cells suggest why these manipulations weaken the inhibitory effect of Ehrenstein boundary contours on the boundary contours of the cross. When the boundary contours of the cross are less inhibited, they can better restrict the diffusion of red-labeled activation. Then the red color can only bleed outside the contours of the cross.

One might ask why the ability of the Ehrenstein boundary contours to inhibit the boundary contours of the cross does not also imply that Ehrenstein boundary contours inhibit contiguous Ehrenstein boundary contours? If they do, then how do any boundary contours survive this process of mutual inhibition? If they do not, then is this explanation of neon color spreading fallacious?
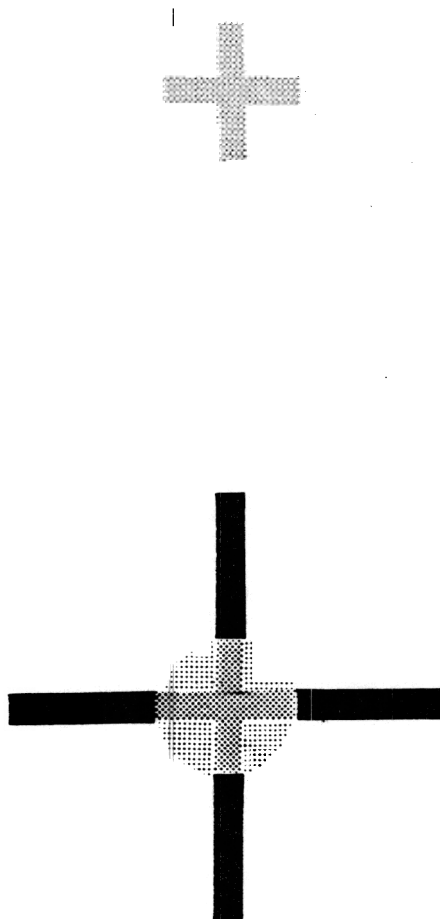

Figure 5. Neon color spreading. ([a] A red cross in isolation appears unremarkable. [b] When the cross is surrounded by an Ehrenstein figure, the red color can flow out of the cross until it hits the illusory contour induced by the Ehrenstein figure.)

Our explanation survives this challenge because the boundary contour process is sensitive to the *amount* of contrast, even though it is insensitive to the *direction* of contrast, as in Figure 1a. Contiguous boundary contours do mutually inhibit one another, but this inhibition is a type of shunting lateral inhibition (Appendix) such that equally strong inhibitory contour signals can remain positive and balanced (Grossberg, 1983a). If, however, the Ehrenstein boundary contour signals are stronger than the boundary contour signals of the cross by a sufficient amount, then the latter signals can be inhibited. This formal property provides an explanation of the empirical fact that neon color spreading is enhanced when the contrast of a figure (e.g., the cross) relative to the background illumination is less than the contrast of the bounding contours (e.g., the Ehrenstein figure) relative to the background illumination (Van Tuijl & de Weert, 1979).

This last point emphasizes one of the paradoxical properties of the boundary contour system that may have delayed its discovery. In order to work properly, boundary contour responses need to be sensitive to the amount of contrast in scenic edges. Despite this contrast sensitivity, boundary contours can be invisible if they do not cause featural contrasts to occur. A large cellular activation does not necessarily have any perceptual effects within the boundary contour system.

Although the rules of the boundary contour system and the feature contour system may prove sufficient to explain neon color spreading, this explanation, in itself, does not reveal the adaptive role of these rules in visual perception. The adaptive role of these rules will become apparent when we ask the following questions: Why does not color spread more often? How does the visual system succeed as well as it does in preventing featural filling-in from flooding every scene? In Section 13, we show how these rules prevent a massive flow of featural quality in response to such simple images as individual lines and corners, not just in response to carefully constructed images like red crosses within Ehrenstein figures. We will now build up to this insight in stages.
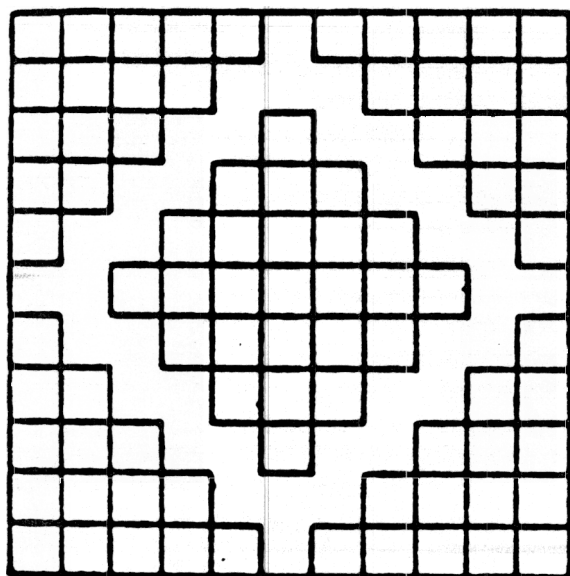
The same concepts also help to explain the complementary color induction that van Tuijl (1975) reported in his original article about the neon effect (Grossberg, 1984a). To see this, draw on white paper a regular grid of horizontal and vertical black lines that form 5 mm squares. Replace a subset of black lines by blue lines. Let this subset of lines be replaced from the smallest imaginary diamond shape that includes complete vertical or horizontal line segments of the grid (Figure 6). When an observer inspects this pattern, the blue color of the lines appears to spread around the blue line segments until it reaches the subjective contours of the diamond shape. This percept has the same explanation as the percept in Figure 5b.
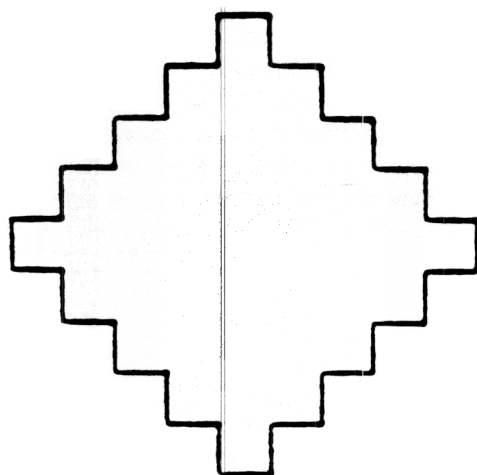
Next replace the black lines by blue lines and the blue lines by black lines. Then the illusory diamond looks yellow rather than blue. Let us suppose that the yellow color in the diamond is induced by the blue lines in the background matrix. Then why in the previous display is not a yellow color in the background induced by the blue lines in the diamond? Why is the complementary color yellow perceived when the background contains blue lines, whereas the original color blue is perceived when the diamond contains blue lines? What is the reason for this asymmetry?

This asymmetry can be explained in the following way. When the diamond is composed of blue lines, then double-opponent color processing enables the blue lines to induce contiguous yellow feature contour signals in the background. These yellow feature contour signals are constrained by the boundary contour signals of the black lines to remain within a spatial domain that also receives feature contour signals from the black lines. The yellow color is thus not seen in the background. By contrast, the boundary contour signals of the black lines in the background inhibit the contiguous boundary contour signals of the blue lines in the diamond. The blue feature contour signals of the blue lines can thus flow within the diamond.

When blue lines form the background, they have two effects on the diamond. They induce yellow feature contour signals via double-opponent processing. They also inhibit the boundary contour signals of the contig-

(a)

(b)

Figure 6. Neon color spreading and complementary color induction. (When the lattice in [a] is composed of black lines and the contour in [b] composed of blue lines is inserted within its diamond-shaped space, then blue color flows within the illusory diamond induced by the black lines. When the lattice in [a] is blue and the contour in [b] is black, then yellow color can flow within the illusory diamond. From "A New Visual Illusion: Neonlike Color Spreading and Complementary Color Induction Between Subjective Contours" by H. F. J. M. van Tuijl. 1975, *Acta Psychologica, 39,* pp. 441–445. Copyright 1975 by North-Holland. Adapted by permission.)

uous black lines. Hence the yellow color can flow within the diamond.

To carry out this explanation quantitatively,

we need to study how double-opponent color processes (light–dark, red–green, yellow–blue) preprocess the feature contour signals from stage MP_L to stage MBC_L and from stage MP_R to stage MBC_R. Double-opponent color processes with the requisite properties can be defined using gated dipole fields (Grossberg, 1980). We also need to quantitatively specify the rules whereby the boundary completion process responds to complex spatial patterns such as grids and Ehrenstein figures. We now approach this task by considering properties of illusory figures.

8. Contrast, Assimilation, and Grouping

The theoretical approach closest in spirit to our is perhaps that of Kennedy (1979). We agree with many of Kennedy's theoretical conclusions, such as

Some kind of brightness manipulation . . . acts on certain kinds of inducing elements but in a way which is related to aspects of form . . . Changes in the luminance of the display have different effects on standard brightness contrast and subjective contour effects . . . Something over and beyond simple brightness contrast is called for. (p. 176)

Grouping factors have to be an essential part of any discussion of subjective contours. (p. 185)

Contrast and grouping factors produce a percept that has some characteristics of a percept of an environmental origin. (p. 189)

Speaking intuitively, Kennedy's remarks about contrast can be compared with properties of our feature contour system, and his remarks about grouping can be compared with properties of our boundary contour system. Once these comparisons are made, however, our theory diverges significantly from that of Kennedy, in part because his theory does not probe the mechanistic level.

For example, Kennedy (1979) invoked two complementary processes to predict brightness changes: contrast and assimilation. Figure 7 describes the assimilation and contrast that are hypothesized to be induced by three shapes. Contrast is assumed to induce a brightening effect and assimilation is assumed to induce a darkening effect. This concept of assimilation is often used to explain how darkness or color can spread throughout an illusory figure (Ware, 1980).

In our theory, local brightening and darkening effects are both consequences of a unified feature contour process. The fact that different parts of a figure induce different relative contrast effects does not imply that different levels of relative contrast are due to different processes. Also, in our theory a darkening effect throughout an illusory figure is not due to a lower relative contrast per se, but to inhibition of a boundary contour leading to diffusion of a darker featural quality throughout the figure. Our theory thus supports the conclusion that perception of relative brightening and darkening effects cannot be explained just using locally defined scenic properties. The global configuration of all

(a)

(b)

(c)

Figure 7. Three shapes redrawn from Kennedy (1979). (Regions of contrast are indicated by [−] signs. Regions of assimilation are indicated by [+] signs. Our theory suggests that the net brightening [contrast] or assimilation [darkening] that occurs between two figures depends not only on figurally induced feature contour signals of variable contrast, but also on the configurationally sensitive boundary contours within which the featurally induced activations can diffuse. From *Perception and Pictorial Representation* [pp. 178–180] edited by C. F. Nodine and D. F. Fisher, 1979. New York: Praeger. Copyright 1979 by Praeger Publishers. Adapted by permission.)

scenic elements determines where and how strongly boundary contours will be generated. Only after these boundary contours are completed can one determine whether the spatial distribution and intensity of all feature contour signals within these boundary contours will have a relative brightening or darkening effect.
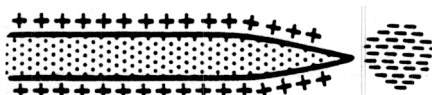
The theory of Kennedy (1979) comes close to this realization in terms of his distinction between brightness and grouping processes. Kennedy suggested, however, that these processes are computed in serial stages, whereas we suggest that they are computed in parallel stages before being joined together (Figure 4). Thus Kennedy (1979, p. 191) wrote

First, there are properties that are dealt with in perception of their brightness characteristics . . . Once this kind of processing is complete, a copy is handed on to a more global processing system. Second, there are properties that allow them to be treated globally and grouped.

Although our work has required new concepts, distinctions, and mechanisms beyond those considered by Kennedy, we find in his work a seminal precursor of our own.

9. Boundary Completion: Positive Feedback Between Local Competition and Long-Range Cooperation of Oriented Boundary Contour Segments
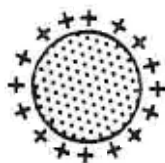
The following discussion employs a series of pictures that elicit illusory contour percepts to suggest more detailed properties of the cooperative boundary completion process of Figure 1d. One or even several randomly juxtaposed black lines on white paper need not induce an illusory contour. By contrast, a series of radially directed black lines can induce an easily perceived circular contour (Figure 8a). This illusory contour is perpendicular to each of the inducing lines. The perpendicular orientation of this illusory contour reflects a degree of orientational specificity in the boundary completion process. For example, the illusory contour becomes progressively less vivid as the lines are tilted to assume more acute angles with respect to the illusory circle (Figure 8b). We explain this tendency to induce illusory contours in the perpendicular direction by combining

properties of the competitive interactions de-
picted in Figures 1b and 1c with properties
of the cooperative process depicted in Figure
1d, just as we did to explain Figure 5b.

It would be mistaken, however, to conclude
that illusory contour induction can take place
only in the direction perpendicular to the
inducing lines. The perpendicular direction
is favored, as a comparison between Figure
8a and Figure 9a shows. Figure 9a differs
from Figure 8a only in terms of the orienta-
tions of the lines; the interior endpoints of
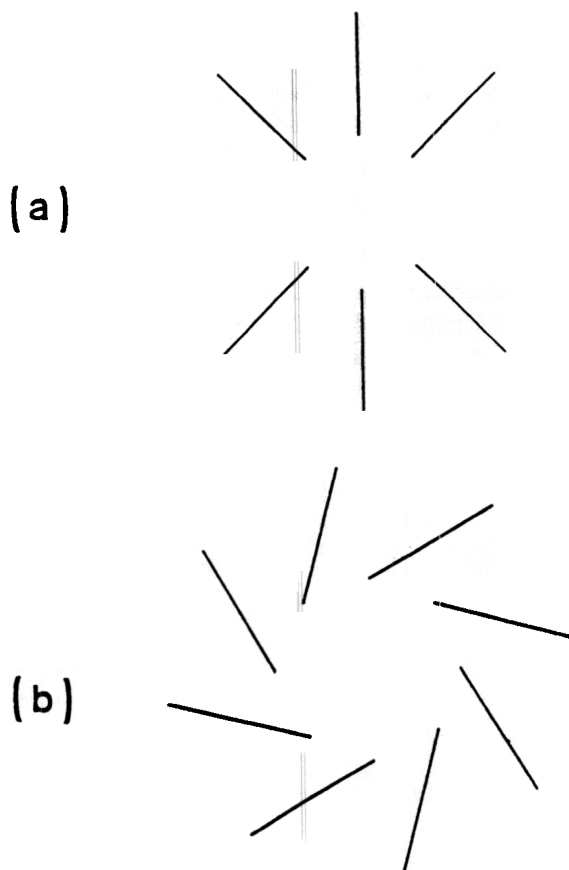the lines are the same. An illusory square is

(a)

(b)

Figure 8. (a) Bright illusory circle induced perpendicular
to the ends of the radial lines. (b) Illusory circle becomes
less vivid as line orientations are chosen more parallel to
the illusory contour. (Thus illusory induction is strongest
in an orientation perpendicular to the ends of the lines,
and its strength depends on the global configuration of
the lines relative to one another. From "Perception and
Pictorial Representation, p. 182, edited by C. F. Nodine
and D. F. Fisher, 1979. New York: Praeger. Copyright
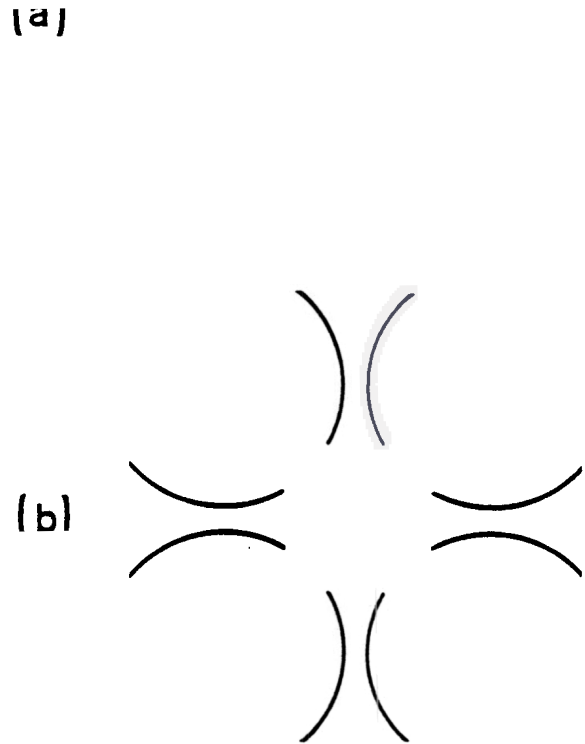1979 by Praeger Publishers. Adapted by permission.)

(a)

(b)

Figure 9. (a) Illusory square generated by changing the
orientations, but not the end-points, of the lines in Figure
8a. (b) Illusory square also generated by lines with
orientations that are not exactly perpendicular to the
illusory contour. (From Perception and Pictorial Repre-
sentation, p. 186, edited by C. F. Nodine and D. F.
Fisher, 1979. New York: Praeger. Copyright 1979 by
Praeger Publishers. Adapted by permission.)

generated by Figure 9a to keep the illusory
contour perpendicular to all the inducing
lines. Not all configurations of inducing lines
can, however, be resolved by a perpendicular
illusory contour. Figure 9b induces the same
illusory square as Figure 9a, but the square
is no longer perpendicular to any of the
inducing lines.

Figures 8 and 9 illustrate several important
points, which we now summarize in more
mechanistic terms. At the end of each induc-
ing line exists a weak tendency for several

approximately perpendicular illusory line segments to be induced (Figure 10a). In isolation, these local reactions usually do not generate a percept of line, if only because they do not define a closed boundary contour that can separate two regions of different relative brightness. Under certain circumstances, these local line segments can interact via the spatially long-range boundary completion process. This cooperative process can be activated by two spatially separated illusory line segments only if their orientations approximately line up across the intervening perceptual space. In Figure 8b, the local illusory line segments cannot line up. Hence no closed illusory contour is generated. In Figure 9b, the local illusory line segments can line up, but only in directions that are not exactly perpendicular to the inducing lines. Thus the long-range cooperative process is orientation-specific across perceptual space (Figure 1d). Boundary completion can be triggered only when pairs of sufficiently strong boundary contour segments are aligned within the spatial bandwidth of the cooperative interaction (Figure 10b).

An important property of Figures 8 and 9 can easily go unnoticed. *Before* boundary completion occurs, each scenic line can induce a band of almost perpendicular boundary contour reactions. This property can be inferred from the fact that each line can generate illusory contours in any of several orientations. Which orientation is chosen depends on the global configuration of the other lines, as in Figures 9a and 9b. An adaptive function of such a band of orientations is clear. If only a single orientation were activated, the probability that several such orientations could be exactly aligned across the perceptual space would be slim. Boundary completion could rarely occur under such demanding conditions.

By contrast, *after* boundary completion occurs, one and only one illusory contour is perceived. What prevents *all* of the orientations in each band from simultaneously cooperating to form a band of illusory contours? Why is not a fuzzy region of illusory contours generated, instead of the unique and sharp illusory contour that is perceived? Somehow the global cooperative process chooses one boundary orientation from among the band of possible orientations at the end of each inducing line. An adaptive function of this process is also clear. It offsets the fuzzy percepts that might otherwise occur in order to build boundaries at all.

How can the coexistence of inducing bands and the percept of sharp boundaries be explained? Given the boundary contour rules
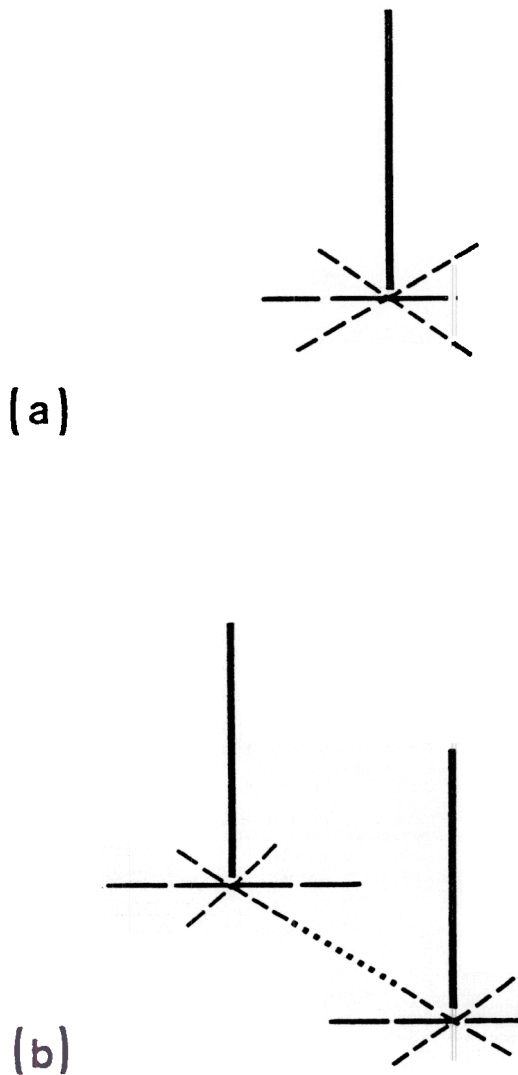

Figure 10. Perpendicular induction. ([a] The end of a scenic line [dark edge] activates a local tendency [dashed lines] to induce contours in an approximately perpendicular direction. [b] If two such local tendencies are sufficiently strong, if they approximately line up across perceptual space, and if they lie within a critical spatial bandwidth, then an illusory contour may be initiated between them.)

depicted in Figure 1, a simple solution is suggested. Suppose that the long-range cooperative process feeds back to its generative boundary contour signals. The several active boundary contour signals at the end of each inducing line are mutually competitive. When positive feedback from the global cooperative process favors a particular boundary contour, then this boundary contour wins the local competition with the other active boundary contour signals. The positive feedback from the global cooperative process to the local competitive process must therefore be strong relative to the mask inputs that induce the band of weak boundary contour reactions at each inducing line end.

Another important property can be inferred from the hypothesis that the boundary completion process feeds back an excitatory signal that helps to choose its own line orientation. How is this positive feedback process organized? At least two local boundary contour signals need to cooperate in order to trigger boundary completion between them. Otherwise, a single inducing line could trigger approximately perpendicular illusory lines that span the entire visual field, which is absurd. Given that two or more active boundary contour signals are needed to trigger the intervening cooperative process, as in Figure 11a, how does the cooperative process span widely separated positions yet generate boundaries with sharp endpoints? Why does not the broad spatial range of the process cause fuzzy line endings to occur, as would a low spatial frequency detector?

Figure 11b suggests a simple solution. First, the two illusory contours generate positive signals along the pathways labeled *1*. These orientationally aligned signals supraliminally excite the corresponding cooperative process, whose nodes trigger positive feedback via pathways such as Pathway 2. Pathway 2 delivers its positive feedback to a position that is intermediate between the inducing line segments. Then, pathways such as 1 and 3 excite positive feedback from intervening pathways such as Pathway 4. The result is a rapid positive feedback exchange between all similarly oriented cooperative processes that lie between the generative boundary contour signals. An illusory line segment is hereby

generated between the inducing line segments, but not beyond them.

10. Boundary Completion as a Statistical Process: Textural Grouping and Object Recognition

Figure 11 shows that the boundary completion process can be profitably thought of as a type of statistical grouping process. In response to a textured scene, many boundary contour segments simultaneously attempt to enhance their local competitive advantage by engaging the positive feedback from all possible cooperative processes that share their spatial position and orientational alignment. As shown in Figure 11b, there exist cooperative processes with multiple spatial band-
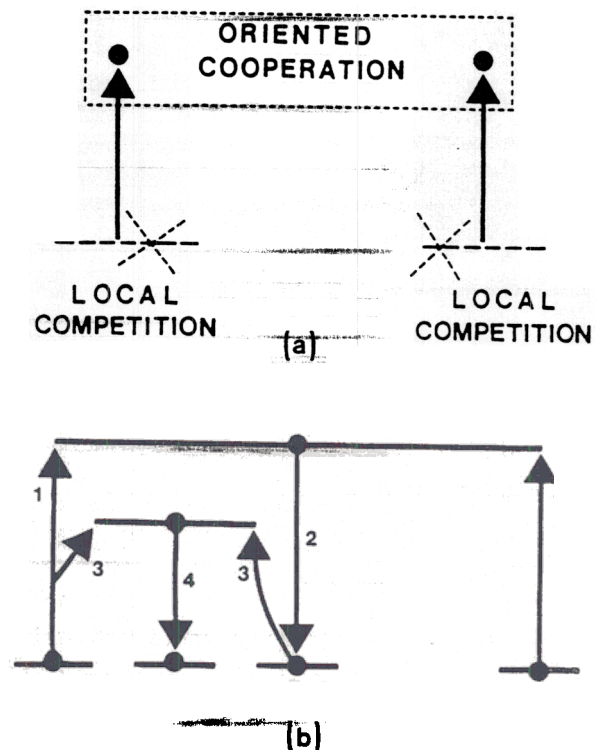

Figure 11. Boundary completion. ([a] Local competition occurs between different orientations at each spatial location. A cooperative boundary completion process can be activated by pairs of aligned orientations that survive their local competitions. [b] The pair of Pathways 1 activate positive boundary completion feedback along Pathway 2. Then pathways such as 3 activate positive feedback along pathways such as 4. Rapid completion of a sharp boundary between Pathways 1 can hereby be generated.)

widths in order to fill in boundary contours between perceptual locations that are separated-by variable distances. The most favorable combination of all positive feedback signals to the competing local boundary contour segments will win the orientational competition (Figure 12), as is illustrated by our simulations below.

The statistical nature of the boundary completion process sheds light on how figures made up of closely spaced dots can be used to induce illusory contours (Kennedy, 1979; Kennedy & Ware, 1978). We also suggest that the orientational tuning and spatially distributed nature of this statistical process
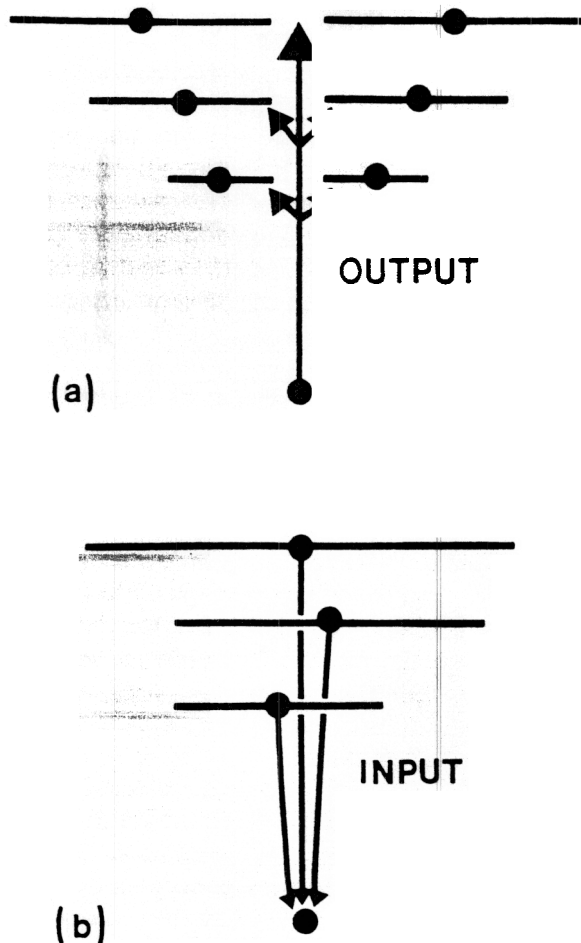

Figure 12. Interactions between an oriented line element and its boundary completion process. ([a] Output from a single oriented competitive element subliminally excites several cooperative processes of like orientation but variable spatial scale. [b] Several cooperative processes of variable spatial scale can simultaneously excite a single oriented competitive element of like orientation.)

contributes to the coherent cross correlations that are perceived using Julesz stereograms (Glass & Switkes, 1976; Julesz, 1971).

These properties of the boundary completion process have been suggested by a consideration of illusory contours. Clearly, however, the process itself cannot distinguish the illusory from the real. The same properties are generated by any boundary contour signals that can win the cooperative–competitive struggle. The ability of the boundary contour process to form illusory groupings enables our theory to begin explaining data from the Beck school (Beck, Prazdny, & Rosenfeld, 1983) on textural grouping, and data of workers like Biederman (1984) and Leeper (1935) concerning how colinear illusory groupings can facilitate or impair recognition of partially degraded visual images (Grossberg & Mingolla, 1985). One of the most important issues concerning the effects of illusory groupings on texture separation and object recognition is the following one. If illusory groupings can be so important, then why are they often invisible? Our theory's distinction between boundary contours and feature contours provides a simple, but radical, answer. Boundary contours, in themselves, are *always* invisible. Perceptual invisibility does not, however, prevent boundary contours from sending large bottom-up signals directly to the object recognition system, and from receiving top-down boundary completion signals from the object recognition system (Grossberg, 1980). Our theory hereby makes a sharp distinction between the elaboration of a visible form percept at the binocular percept (BP) stage (Figure 4) and the activation of object recognition mechanisms. We suggest that these two systems are activated in parallel by the BCS stage.

The above discussion suggests some of the properties whereby cooperative interactions can sharpen the orientations of boundary contour segments as they span ambiguous perceptual regions. This discussion does not, however, explain why illusory contour segments are activated in bands of nearly perpendicular orientations at the ends of lines. The next section supplies some further information about the process of illusory induction. The properties of this induction process will again hold for both illusory and real

contours, which exist on an equal mechanistic footing in the network.

11. Perpendicular Versus Parallel Contour Completion

The special status of line endings is highlighted by consideration of Figure 2a. In this famous figure, four black pac-man forms generate an illusory Kanizsa square. The illusory edges of the Kanizsa square are completed in a direction parallel to the the dark–light inner edges of the pac-man forms. Why are *parallel* orientations favored when black pac-man forms are used, whereas *perpendicular* orientations are favored when the ends of black lines are used? Figure 13a emphasizes this distinction by replacing the black pac-man forms with black lines whose endpoints are perpendicular to the illusory contour. Again the illusory square is easily seen, but is now due to perpendicular induction rather than to parallel induction.

An analysis of spatial scale is needed to understand the distinction between perpendicular induction and parallel induction. For example, join together the line endpoints in Figure 13a and color the interiors of the resultant closed contours black. Then an illusory square is again seen (Figure 13b). In Figure 13b, however, the illusory contours are parallel to the black closed edges of the bounding forms, rather than perpendicular
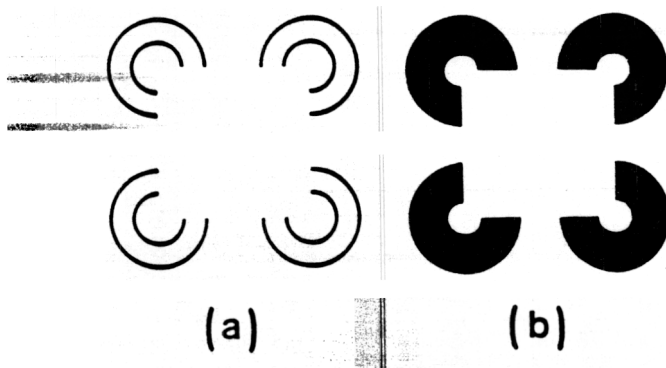

Figure 14. Influence of figural contrast on illusory brightness. (When the black interiors of Figure 13b are colored white, the illusory square is no longer perceived.)

to the ends of lines, as in Figure 13b. The black forms in Figure 13b can be thought of as thick lines. This raises the question: How thick must a line become before perpendicular induction is replaced by parallel induction? How thick must a line become before its "open" end becomes a "closed" edge? In our networks, the measure of thickness is calibrated in terms of several interacting parameter choices: the number of degrees spanned by an image on the retina, the mapping from retinal cells to oriented masks within the boundary contour system, the spatial extent of each oriented mask, and the spatial extent of the competitive interactions that are triggered by outputs from the oriented masks.

The subtlety of this calibration issue is illustrated by Figure 14. In Figure 14, the black interiors of the inducing forms in Figure 13b are eliminated, but their boundaries are retained. The black contours in Figure 13b remain closed, in a geometrical sense, but the illusory square vanishes. Does this mean that these black contours can no longer induce an illusory square boundary contour? Does it mean that an illusory square boundary contour does exist, but that the change in total patterning of feature contour signals no longer differentially brightens the inside or outside of this square? Or is a combination

(a)   **(b)**

Figure 13. Open versus closed scenic contours. ([a] If the black pac-man figures of Figure 2 are replaced by black lines of perpendicular orientation, then a bright illusory square is seen. [b] If line ends are joined together by black lines and the resultant closed figures are colored black, then a bright illusory square is again seen. These figures illustrate how perpendicular contour induction by *open* line ends can be replaced by parallel contour induction by *closed* edges.)
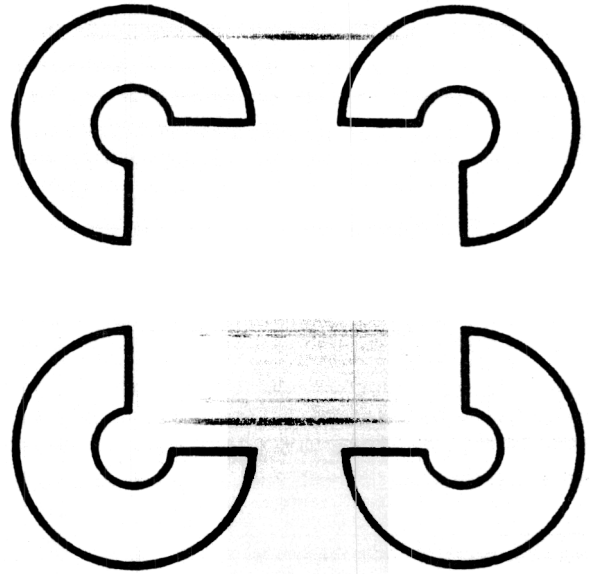
of these two types of effects simultaneously at work? Several spatial scales are simultaneously involved in both the boundary contour process and the feature contour process. A quantitative analysis of multiple scale interactions goes beyond the scope of this article. The following discussion outlines some factors that are operative within each spatial scale of the model.

Section 13 suggests that both perpendicular induction and parallel induction are properties of the same boundary completion process. The different induction properties are traced to different reactions of the boundary completion process to different visual patterns. Before exploring these points, the following section clarifies how removal of the black interiors in Figure 14 eliminates the percept of an illusory Kanizsa square.

12. Spatial Scales and Brightness Contrast

Figure 15 uses pac-man forms instead of the forms in Figure 14 due to their greater simplicity. In Figure 15 the interiors of the upper two pac-man forms are black, but the

Figure 16. Effects of spatial scale on perceived contrast. ([a] No obvious brightness difference occurs between the inside and the outside of the circle. [b] By thickening the circle sufficiently, it becomes a background annulus. The interior of the circle can then be brightened by classical brightness contrast.)
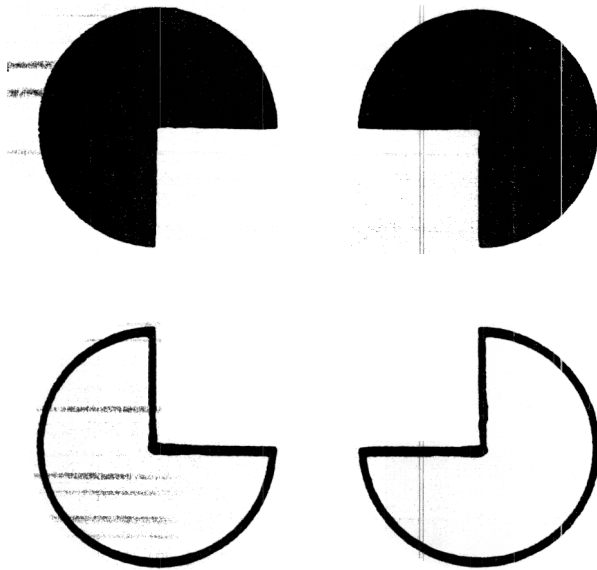

Figure 15. Influence of figural contrast on illusory brightness. (If only two pac-man forms in Figure 2 are colored black, and the other two forms have white interiors, then an illusory contour can be seen between contiguous black and white forms. This percept suggests that some illusory boundary contour induction may occur in response to Figure 14, but that not enough differential feature contour contrast is generated inside and outside the boundary contour to make the boundary contour visible.)

interiors of the bottom two pac-man forms are white. When all four pac-man forms are colored white, an illusory square is not visible, just as in Figure 14. In Figure 15, by contrast, two vertical illusory contours can be perceived between the black pac-man forms and the pac-man forms with white interiors. The existence of these vertical contours suggests that the vertical black lines in the bottom two pac-man figures can cooperate with the vertical black lines in the top two pac-man figures to induce boundary contours in a direction parallel to their orientation. When all the pac-man forms have white interiors, however, the interior contrast generated by these forms by the feature contour process does not differ significantly from the exterior contrast that is generated by these forms. By using two pac-man forms with black interiors, the interior contrast is enhanced relative to the exterior contrast. This enhanced interior brightness flows downward within the illusory vertical contours, thereby enhancing their visibility.

Why does coloring the interiors of two pac-man figures black enhance their interior contrastive effect? This property can be better understood by comparing it with classical demonstrations of brightness contrast. This comparison shows that the property in question is not peculiar to illusory figures. It is the same property as the brightness contrast that is due to "real" figures.

Figure 16 compares a thin letter O with a thick letter O. The brightness levels interior to and exterior to the thin letter O are not obviously different. A sufficiently thick letter O can generate a different percept, however.

If the letter O is made sufficiently thick, then it becomes a black annulus surrounding a white circle. It is well-known from classical studies of brightness contrast that darkening an annulus around an interior circle can make the circle look brighter (Cornsweet, 1970). We suggest that the difference between a thin letter O and a brightness contrast demonstration reflects the same process of lateral inhibition (Grossberg, 1981) as the difference between a pac-man form with white interior and a pac-man form with black interior.

13. Boundary–Feature Trade-Off: Orientational Uncertainty and Perpendicular End Cutting

We are now ready to consider the boundary–feature trade-off and to show how it explains the paradoxical percepts above as consequences of an adaptive process of fundamental importance.

The theory's rules begin to seem natural when one acknowledges that the rules of each contour system are designed to offset insufficiencies of the other contour system. The boundary contour system, by itself, could at best generate a perceptual world of outlines. The feature contour system, by itself, could at best generate a world of formless qualities. Let us accept that these deficiencies are, in part, overcome by letting featural filling-in spread over perceptually ambiguous regions until reaching a boundary contour. Then it becomes a critical task to synthesize boundary contours that are capable of restraining the featural flow at perceptually important scenic edges.

Orientationally tuned input masks, or receptive fields, are needed to initiate the process of building up these boundary contours (Figure 1). If the directions in which the boundaries are to point were not constrained by orientational tuning, then the process of boundary completion would become hopelessly noisy. We now show that orientationally tuned input masks are insensitive to orientation at the ends of scenic lines and corners. A compensatory process is thus needed to prevent featural quality from flowing out of the percepts of all line endings and corners. Without this compensatory process, filling-in
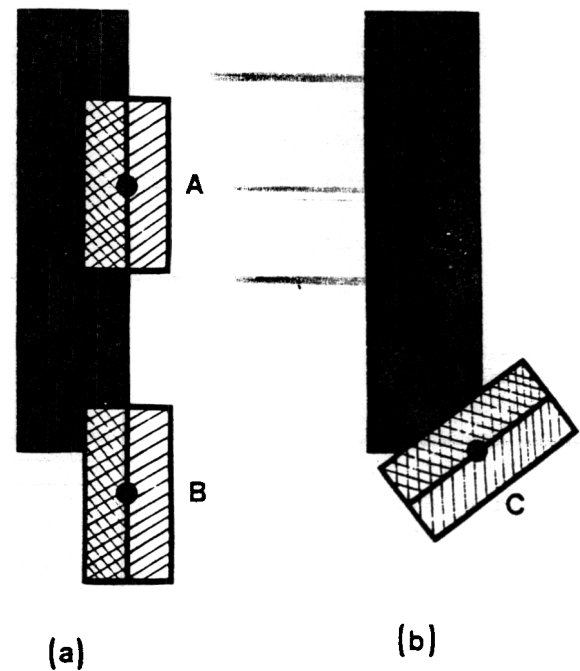

(a)   (b)

Figure 17. Orientational specificity at figural edges, corners, and exteriors. ([a] At positions such as A that are along a figural edge, but not at a figural corner, the oriented mask parallel to the edge is highly favored. At positions beyond the edge, such as B, masks of the same orientation are still partially activated. This tendency can, in the absence of compensatory mechanisms, support a flow of dark featural activity down and out of the black figure. [b] A line is thin, functionally speaking, when at positions near a corner, such as C, many masks of different orientations are all weakly activated or not activated at all.)

anomalies like neon color spreading would be ubiquitous. This compensatory process is called the *end-cutting* process.

The end-cutting process is the net effect of the competitive interactions described in Figure 1b and 1c. Thus the rules of the boundary contour system take on adaptive meaning when they are understood from the viewpoint of how boundary contours restrict featural filling-in. This section discusses how this end-cutting process, whose function is to build up "real" boundary contours with sharply defined endpoints, can also sometimes generate illusory boundary contours through its interaction with the cooperative boundary completion process of Figure 1d and Figure 11.

The need for an end-cutting process can be seen by considering Figure 17. Figure 17 describes a magnified view of a black vertical line against a white background. Consider

Position A along the right edge of the scenic line. A vertically oriented input mask is drawn surrounding Position A. This mask is sensitive to the relative contrast of line edges that fall within its elongated shape. The mask has been drawn with a rectangular shape for simplicity. The rectangular shape idealizes an orientationally sensitive receptive field (Hubel & Wiesel, 1977). The theory assumes that a sufficiently contrastive vertical dark–light edge or a sufficiently contrastive light–dark edge falling within the mask area can activate the vertically tuned nodes, or cells, that respond to the mask at Position A. These cells are thus sensitive both to orientation and to the amount of contrast, but not to the direction of contrast (Figure 1a). A set of masks of varying orientations is assumed to exist at each position of the field. Each mask is assumed to have an excitatory effect on cells that are tuned to the same orientation and an inhibitory effect on cells that are tuned to the other orientations at its spatial position (Figure 1c).

At a position, such as A, which lies along a vertical edge of the line far from its end, the rules for activating the oriented masks imply that the vertical orientation is strongly favored in the orientational competition. A tacit hypothesis is needed to draw this conclusion: The oriented masks are elongated enough to sense the spatially anisotropic distribution of scenic contrast near Position A. Were all the masks circularly symmetric, no mask would receive a larger input than any other.

When oriented masks are activated at a position such as B, a difficulty becomes apparent. Position B lies outside the black line, but its vertical mask still overlaps the black inducing line well enough to differentially activate its vertically tuned cells. Thus the possibility of selectively registering orientations carries with it the danger of generating boundary contours that extend beyond their inducing edges. Suppose that the vertically oriented cells at positions such as B were allowed to cooperate with vertically oriented cells at positions such as A. Then a vertical boundary contour could form that would enable featural quality to flow out of the line. We now show that the end-cutting process that prevents this from happening also has

properties of illusory induction that have been described above.

Suppose that inhibitory signals can be generated from positions such as A to positions such as B that lie beyond the end of the line. Because the position of the line relative to the network can change unpredictably through time, these signals need to be characterized in terms of the internal network geometry rather than with respect to any particular line. To prevent featural flow, the vertical activation at Position A needs to inhibit the vertical activation at Position B, but not all activations at Position B. Thus the inhibitory process is orientationally selective across perceptual space (Figure 1b). The spatial range of the inhibitory process must also be broad enough for vertical activations at line positions such as A to inhibit vertical activations at positions such as B that lie outside the line. Otherwise expressed, the spatial range of these orientationally selective inhibitory signals must increase with the spatial scale of the masks.

Once the need for an inhibitory end cutting process is recognized, several paradoxical types of data immediately become more plausible. Consider, for example, Figure 5b in which the vertical boundary contours of the Ehrenstein figure inhibit the vertical boundary contours of the contiguous red cross. The orientational specificity and limited spatial bandwidth of the inhibition that are needed to prevent featural flow also explain why increasing the relative orientation or spatial separation of the cross and Ehrenstein figure weakens the neon spreading effect (Redies & Spillmann, 1981).

The inhibitory end-cutting process explains how a vertical orientation of large contrast at a position such as A in Figure 17a can inhibit a vertical orientation of lesser contrast, as at Position B. More than this inhibitory effect is needed to prevent featural activity from flowing outside of the line. Horizontally oriented boundary contours must also be activated at the end of the line. These horizontal boundary contours are not activated, however, without further network machinery.

To understand why this is so, consider Position C in Figure 17b. Position C lies at the end of a narrow black line. Due to the thinness of the line relative to the spatial

scale of the oriented input masks, several oriented masks of differing orientations at Position C can all register small and similar amounts of activation, as in the computer simulations of Section 17. Orientational selectivity breaks down at the ends of lines, even though there may exist a weak vertical preference. After the strongly favored vertical orientation at Position A inhibits the weakly activated vertical orientation at positions such as B or C, the mask inputs themselves do not provide the strong activations of horizontal orientations that are needed to prevent featural flow. Further processing is needed.

The strong vertical inhibition from Position A must also disinhibit horizontal, or close-to-horizontal, orientations at positions such as B and C. This property follows from the postulate that perpendicular orientations compete at each perceptual position, as in Figure 1c. Thus the same competitive mechanisms in Figure 1b and 1c that explain how end cutting—with its manifestly adaptive function—occurs, also explain how red color can paradoxically flow out of a red cross when it is surrounded by an Ehrenstein figure (Figure 5).

As the thickness of the black line in Figure 17 is increased, the horizontal bottom positions of the line begin to favor horizontal orientations for the same reason that the vertical side positions of the line favor vertical orientations. When this occurs, the horizontal orientations along the thickened bottom of the line can cooperate better via the boundary completion process to directly form a horizontal boundary contour at the bottom of the figure. Parallel induction by a thick black form hereby replaces perpendicular induction by a thin black line as the thickness of the line is increased.

14. Induction of "Real" Contours Using "Illusory" Contour Mechanisms

Some readers might still be concerned by the following issue. Does not the end-cutting process, by preventing the vertical boundary contour from extending beyond Position C in Figure 17b, create an even worse property: the induction of horizontal illusory contours? Due to the importance of this issue in our theory, we summarize the adaptive value of

this property using properties of the cooperative boundary completion process of Figure 1d and Figure 11.

Suppose that inhibition from Position A to Position B does not occur in Figure 17a. Then vertical activations can occur at both positions. By Figure 11, an illusory vertical boundary contour may be generated beyond the "real" end of the line. The same is true at the left vertical edge of the line. Due to the existence of ambiguous boundary contour orientations between these vertical boundary contours, featural quality can freely flow between the dark interior of the line and the white background below.

The end-cutting process prevents featural flow from occurring at line ends. It does so by generating a strong horizontal activation near corner positions such as C in Figure 17b. In the same way, it generates a strong horizontal activation near the bottom left corner of the line. Using the cooperative process in Figure 11, these two horizontal activations can activate a horizontal boundary contour across the bottom of the line. Although this horizontal boundary contour is "illusory," it prevents the downward flow of dark featural quality beyond the confines of the inducing line, and thereby enables the network to perceive the line's "real" endpoint. Thus the "real" line end of a thin line is, strictly speaking, an "illusory" contour. "Real" and "illusory" contours exist on an equal ontological footing in our theory.

In the light of this adaptive interaction between the competitive end-cutting process and the cooperative boundary completion process in the perception of "real" scenic contours, the fact that occasional juxtapositions of "real" scenic contours also generate boundary contours that are judged to be "illusory" seems to be a small price to pay.

The remaining sections of this article describe a real-time network that is capable of computing these formal properties.

15. Gated Dipole Fields

We assume that the competitive end-cutting and cooperative boundary completion processes are mediated by interactions between on-cells and off-cells that form opponent processes called *gated dipoles*. Specialized net-

works, or fields, of gated dipoles have been used to suggest explanations of many visual phenomena, such as monocular and binocular rivalry, spatial frequency adaptation, Gestalt switching between ambiguous figures, color-contingent and orientation-contingent after-effects, and attentional and norepinephrine influences on visual critical period termination and reversal (Grossberg, 1976, 1980, 1982, 1983a, 1984a). The gating properties of these fields are described here only in passing.

Before describing the details of the gated dipole fields that will be used, we qualitatively summarize how they can mediate the competitive end-cutting process. Several closely related variations of this design can generate the desired properties. We develop one scheme that incorporates the main ideas. Suppose that an input mask at Position (i, j) is preferentially tuned to respond to an edge of orientation k. Denote the input generated by this mask by J_{ijk}. Suppose that this input activates the potential x_{ijk} of the corresponding on-cell population. Also suppose that the variously oriented inputs J_{ijk} at a fixed position (i, j) cause a competition to occur among the corresponding on-cell potentials x_{ijk}. In the present scheme, we suppose that each orientation k preferentially inhibits the perpendicular orientation K at the same position (i, j). In this sense, the on-potential x_{ijK} is the off-potential of the input J_{ijk}, and the on-potential x_{ijk} is the off-potential of the input J_{ijK}. These pairs of competing potentials define the dipoles of the field.

One consequence of dipole competition is that at most one potential x_{ijk} or x_{ijK} of a dipole pair can become supraliminally active at any time. Furthermore, if both inputs J_{ijk} and J_{ijK} are equally large, then—other things being equal—neither potential x_{ijk} or x_{ijK} can become supraliminally active. Dipole competition between perpendicular orientations activates a potential x_{ijk} or x_{ijK} only if it receives a larger net input than its perpendicularly tuned competitor. The amount of activation is, moreover, sensitive to the relative contrast of these antagonistic inputs.

An oriented input J_{ijk} excites its own potential x_{ijk} and inhibits similarly oriented potentials x_{pqk} at nearby positions (p, q), and conversely. The input masks are thus orga-nized as part of an on-center off-surround anatomy of short spatial range (Figure 18). Due to this convergence of excitatory and inhibitory inputs at each orientation and position, the net input to a potential x_{ijk} may be excitatory or inhibitory. This situation creates a new possibility. Suppose that x_{ijk} receives a net inhibitory input, whereas x_{ijK} receives no external input. Then x_{ijk} is inhib-ited and x_{ijK} is supraliminally excited. This activation of x_{ijK} is due to a disinhibitory action that is mediated by dipole competition. In order for x_{ijK} to be excited in the absence of an excitatory input J_{ijK}, a persistently active, or tonic, internal input must exist. This is another well-known property of gated dipoles (Grossberg, 1982). By symmetry, the same tonic input influences each pair of potentials x_{ijk} and x_{ijK}.

When transmitter gates are placed in spe-cialized dipole pathways—hence the name *gated dipole*—properties like negative afteref-fects, spatial frequency adaptation, and bin-ocular rivalry are generated (Grossberg, 1980, 1983a, 1983b). Transmitter gates are not further discussed here.

We now apply the properties of dipole competition to explain the inhibitory end-cutting process in more quantitative detail. Suppose that vertical input masks J_{pqk} are preferentially activated at positions such as A in Figure 17a. These input masks succeed in activating their corresponding potentials x_{pqk}, which can then cooperate to generate a vertically oriented boundary contour.

By contrast, positions such as B and C in Figure 17 receive orientationally ambiguous inputs due to the thinness of the black bar relative to the length of the oriented masks. Consequently, the inputs J_{ijk} to these positions near the end of the bar are small, and several mask orientations generate inputs of compa-rable size. Without compensatory mecha-nisms, featural quality would therefore flow from the end of the bar.

This is prevented from happening by the vertically oriented input masks J_{pqk} at posi-tions such as A. These input masks generate large off–surround inhibitory signals to x_{ijk} at positions (i, j) at the end of the bar. Due to dipole competition, the horizontally tuned potentials x_{ijK} are disinhibited. The horizon-tally tuned potentials of several horizontally

aligned positions at the end of the bar can then cooperate to generate a horizontally oriented boundary contour that prevents featural quality from flowing beyond the end of the bar.

16. Boundary Completion: Oriented Cooperation Among Multiple Spatial Scales

The stage of dipole competition between perpendicular orientations is followed by a stage of shunting competition among all the orientations corresponding to a fixed position (i, j). The stage of shunting competition possesses several important properties. For one, the shunting competition tends to conserve, or normalize, the total activity of the

potentials y_{ijk} at the final stage of competitive processing

$$\sum_{k=1}^{n} y_{ijk}$$

(Figure 18). This limited capacity property converts the activities $(y_{ij1}, y_{ij2}, \ldots, y_{ijn})$ of the final stage into a ratio scale. See the Appendix for mathematical details.

An equally important property of the shunting competition at each position (i, j) becomes apparent when several positions cooperate to complete boundary contours. Figure 19 depicts how two properly aligned potentials, y_{ijk} and y_{uvk}, of orientation k at different positions (i, j) and (u, v) cooperate to activate the potential z_{pqk} at an intervening

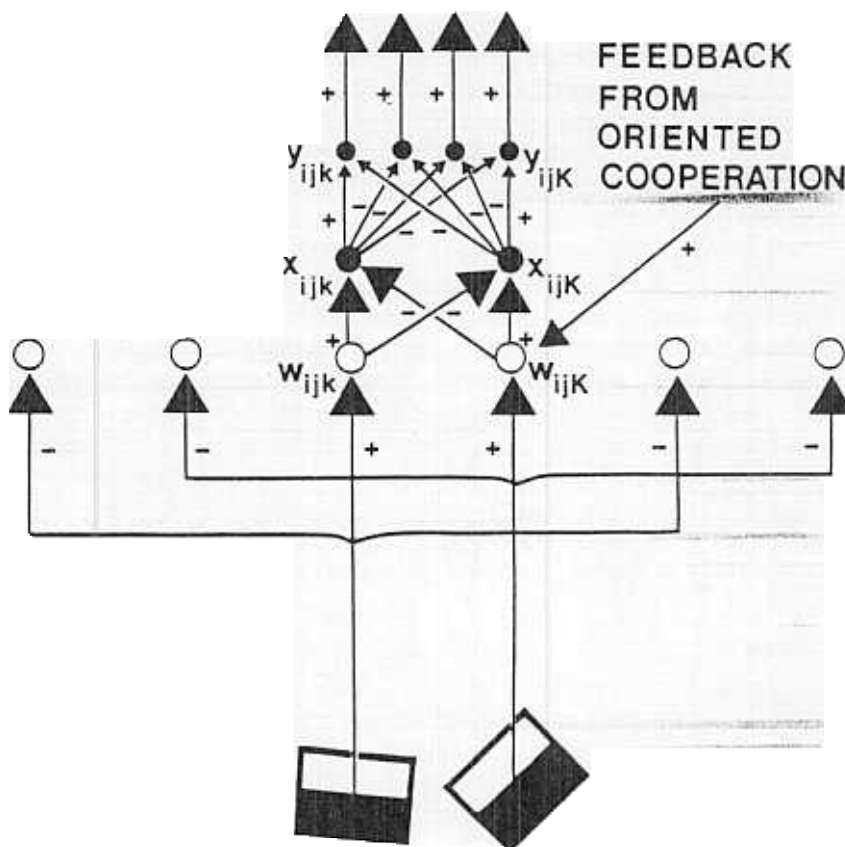## INPUT TO ORIENTED
COOPERATION

Figure 18. Orientationally tuned competitive interactions. (A shunting on-center off-surround interaction within each orientation and between different positions is followed by a push-pull dipole competition between orientations and within each position. The different orientations also compete to normalize the total activity within each position before eliciting output signals to the cooperative boundary completion process that exists between positions whose orientations are approximately aligned.)
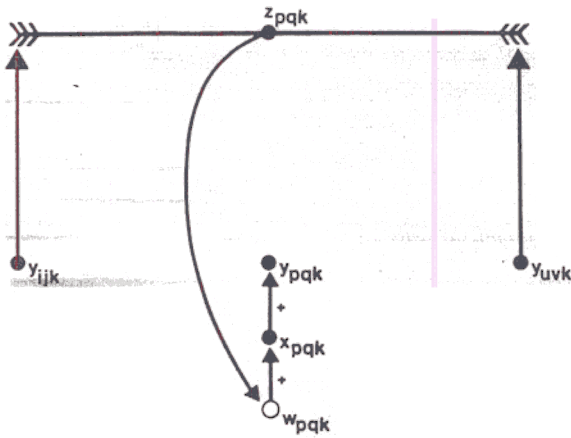
Figure 19. Excitatory boundary completion feedback between different positions. (Outputs triggered by aligned dipole on-potentials y_{ijk} and y_{uvk} can activate intervening boundary completion potentials z_{pqk}. The potentials z_{pqk}, in turn, deliver strong positive feedback to the corresponding potentials w_{pqk}, which thereupon excite the potentials x_{pqk} and inhibit the potentials x_{pqK}.)

position (p, q). Potential z_{pqk}, in turn, excites the potential x_{pqk} of the same orientation k and at the same position (p, q). As in Figure 11, this positive feedback process rapidly propagates to the potentials of orientation k corresponding to all positions between (i, j) and (u, v).

To generate a sharp contour (Section 9), a single orientation k needs to be chosen from among several partially activated orientations at each position (p, q). Such a choice is achieved through an interaction between the oriented cooperation and the shunting competition. In particular, in Figure 19, the positive feedback from z_{pqk} to x_{pqk} enhances the relative size of y_{pqk} compared to its competitors y_{pqr} at Position (p, q). In order for the positive feedback signals $h(z_{pqk})$ from z_{pqk} to x_{pqk} to achieve a definite choice, the form of the signal function $h(w)$ must be correctly chosen. It was proved in Grossberg (1973) that a signal function $h(w)$ that is faster-than-linear at attainable activities $w = z_{pqk}$ is needed to accomplish this task. A faster-than-linear signal function sharply contrast-enhances the activity patterns that reverberate in its positive feedback loops (Grossberg, 1983a). Examples of faster-than-linear signal functions are power laws such as $h(w) = Aw^n$, $A > 0$, $n > 1$; threshold laws such as

$h(w) = A \max(w - B, 0)$, $A > 0$, $B > 0$; and exponential laws such as $h(w) = Ae^{Bw}$, $A > 0$, $B > 0$. The opponent competition among the potentials x_{ijk} and the normalizing competition among the potentials y_{ijk} may be lumped into a single process (Grossberg, 1983a). They have been separated herein to achieve greater conceptual clarity.

7. Computer Simulations

This section describes some of the simulations that have been done in our ongoing program of quantitative model testing and refinement. The equations that govern the simulations are defined in the Appendix.

Figure 20 describes a simulation of boundary completion. In this simulation, the potentials of gated dipoles at Positions 15 and 25 receive positive inputs. The potential of the gated dipole at Position i is denoted by $y_i(t)$ in Figure 20. A single positional index i is sufficient because the simulation is carried out on a one-dimensional array of cells. The potential of the boundary completion cell at Position i is denoted by $z_i(t)$. Figure 20 provides a complete summary of how the boundary completion process unfolds through time. Each successive increasing curve in the figure describes the spatial pattern of activities $y_i(T)$ or $z_i(T)$ across Positions i at successive times $t = T$. Note that the input to the two gated dipole positions cause a rapid activation of gated dipole positions that lie midway between them via cooperative feedback signals. Then these three positions rapidly fill in the positions between them. The final pattern of y_i activities defines a uniformly active boundary that ends sharply at the inducing Positions 15 and 25. By contrast, the final pattern of z_i values extends beyond the inducing positions due to subliminal activation of these positions by the interactions depicted in Figure 12a.

Figure 21 illustrates how the boundary completion process attenuates scenic noise and sharpens fuzzy orientation bands. Each column of the figure describes a different time during the simulation. The original input is a pattern of two noisy but vertically biased inducing sources and a horizontally oriented noise element. Horizontally biased end cuts
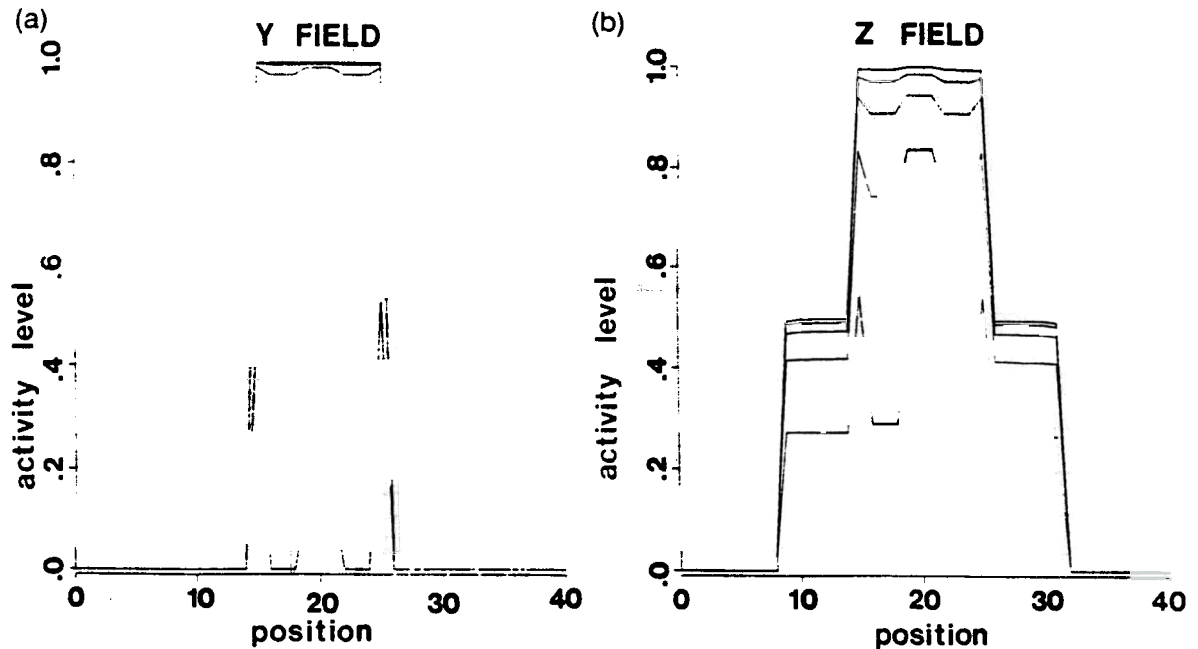
Figure 20. Computer simulation of boundary completion in a one-dimensional array of cells. (Two sustained inputs to Positions 15 and 25 of the *y* field trigger a rapid filling-in. Activity levels at five successive time periods are superimposed, with activity levels growing to a saturation level. [a] Sharp -boundary in *y* field of Figure 19. [b] Fringe of subliminal activity flanks suprathreshold activity pattern in *z* field of Figure 19.)

are momentarily induced before the oriented cooperation rapidly attenuates all nonvertical elements to complete a vertical boundary contour.

Figures 22a and 22b illustrate how a field of oriented masks, such as those depicted in Figure 17, react to the sharp changes in direction at the end of a narrow input bar. These figures encode the activation level of each mask by the length of the line having the same orientation as the mask at that position. We call such a display an *orientation field.* A position at which only one line appears is sensitive only to the orientation of that line. A position at which several lines of equal length appear is equally sensitive to all these computed orientations. The relative lengths of lines across positions encode the relative mask activations due to different parts of the input pattern.

Figure 22a shows that a strong vertical preference exists at positions along a vertical edge that are sufficiently far from an endpoint (e.g., positions such as A in Figure 17a). Masks with close-to-vertical orientations can

also be significantly activated at such positions. Thus there exists a strong tendency for parallel induction of contours to occur along long scenic edges, as in the illusory Kanizsa square of Figure 2.

This tendency for strong parallel induction to occur depends on the length of the figural edge relative to the length of the input masks. Consider, for example, positions along the bottom of the figure, such as Position C in Figure 17b. Because the figure is narrow relative to the mask size, the orientational preferences are much weaker and more uniformly distributed, hence more ambiguous, at the ends of narrow lines.

Figure 22b illustrates how different values of mask parameters can generate different orientation fields in response to the same input pattern. The dark–light and light–dark contrast that is needed to activate a mask (parameter α in the Appendix, Equation A1) is higher in Figure 22b than in Figure 22a. Consequently the positions that respond to scenic edges are clustered closer to these edges in Figure 22b, and edge positions near
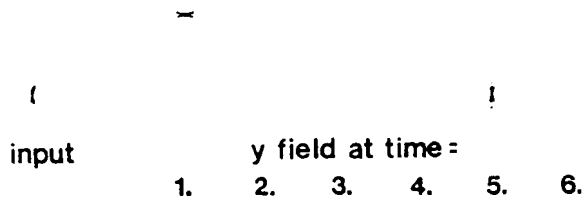
REAL TIME BOUNDARY COMPLETION

input   y field at time =
          1.   2.   3.   4.   5.   6.

Figure 21. Each column depicts a different time during the boundary completion process. (The input consists of two noisy but vertically biased inducing line elements and an intervening horizontal line element. The competitive–cooperative exchange triggers transient perpendicular end cuts before attenuating all nonvertical elements as it completes the vertical boundary.)

the line end are not activated. In both Figures 22a and 22b, the input activations near the line end are weak, orientationally ambiguous, or nonexistent.

In Figures 23a and 23b, the orientation fields of Figures 22a and 22b are transformed by the competitive interactions within a dipole field. The functional unit of this field again consists of a complete set of orientations at each perceptual location. At each position (i, j), the value y_{ijk} of the final competitive stage (Figure 18) is described by a line of orientation k whose length is proportional to y_{ijk}. In response to the orientation field of Figure 22a, the dipole field generates a strong horizontal end cut in Figure 23a at the perceptual

positions corresponding to the end of the line. These horizontal activations can cooperate to generate a boundary contour capable of preventing featural flow from the end of the line. Oblique activations are also generated near the line end as part of this complementary induction process. These oblique activations can induce nonperpendicular illusory contours, as in Figure 9b.

In Figure 23b, "illusory" horizontal end cuts are generated at the locations where the vertically oriented inputs of Figure 22b terminate, despite the fact that the locations do not coincide with the end of the line. Comparison of Figures 23a and 23b shows that the horizontal end cuts in both examples exist on a similar ontological footing, thereby clarifying the sense in which even the percepts of "real" line ends are "illusory" and the percepts of "illusory" line ends are "real." This conclusion does not imply that human observers are unable to say when certain illusory boundaries seem to be "unreal." We trace this capability to the different ways in which some scenes coactivate the feature contour system and the boundary contour system, rather than to different boundary completion mechanisms within the boundary contour system for "real" and "illusory" line percepts.

18. Brightness Paradoxes and the Land Retinex Theory

This article has focused on the process whereby both real and illusory visual contours are formed. From the perspective of this process, the distinction between a real contour and an illusory contour is highly ambiguous. The role of end cutting in defining sharp "illusory" boundary contours at the "real" ends of narrow lines is a case in point (Section 14).
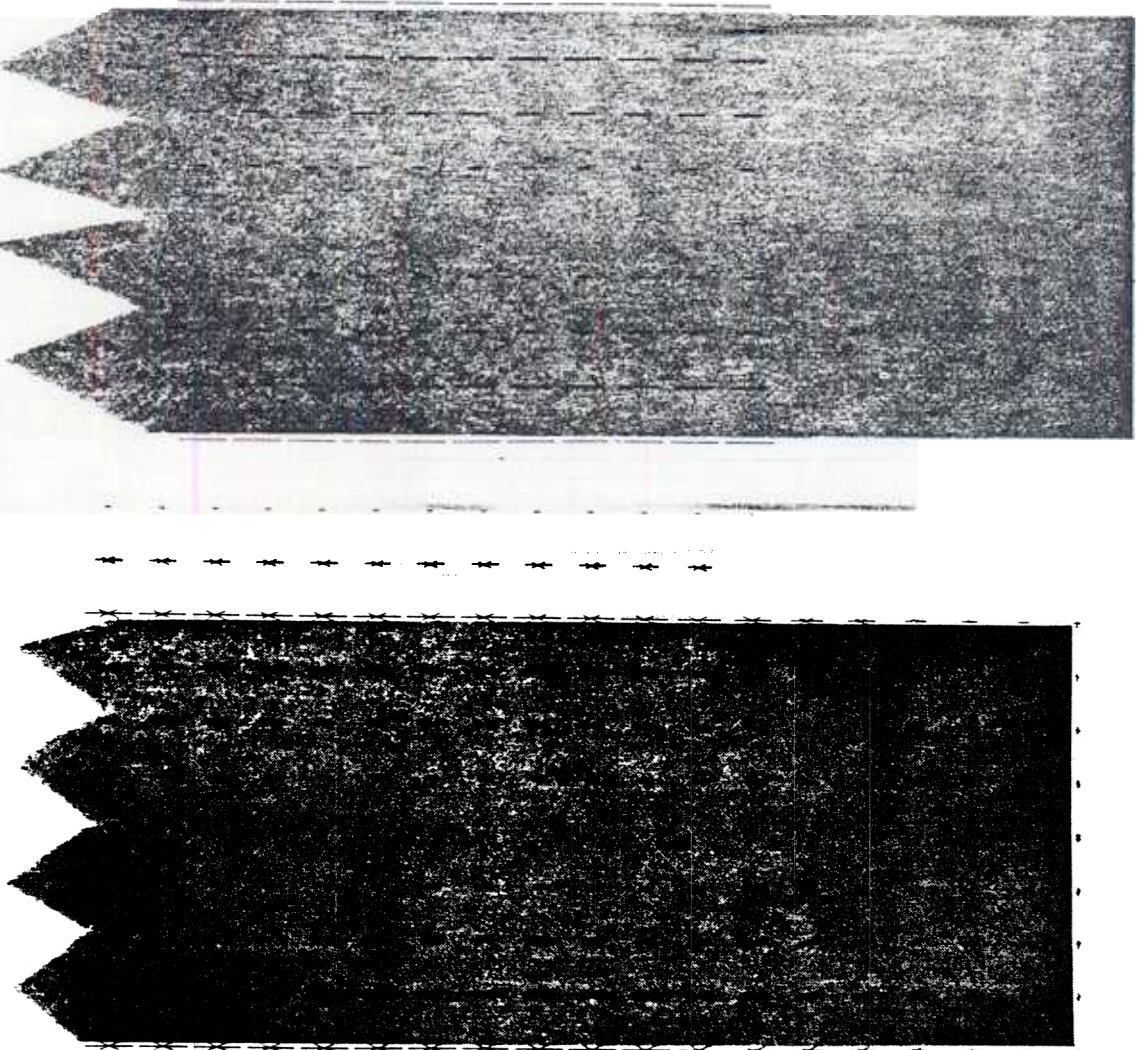
To quantitatively understand illusory brightness effects in the theory, it is necessary to analyze how feature contour signals combine

Figure 22. (a) Orientation field. (Lengths and orientations of lines encode relative sizes of activations and orientations of the input masks at the corresponding positions. The input pattern corresponds to the shaded area. Each mask has total exterior dimensions of 16×8 units, with a unit length being the distance between two adjacent lattice positions.) (b) Orientational field whose masks respond to higher contrasts than those in (a).
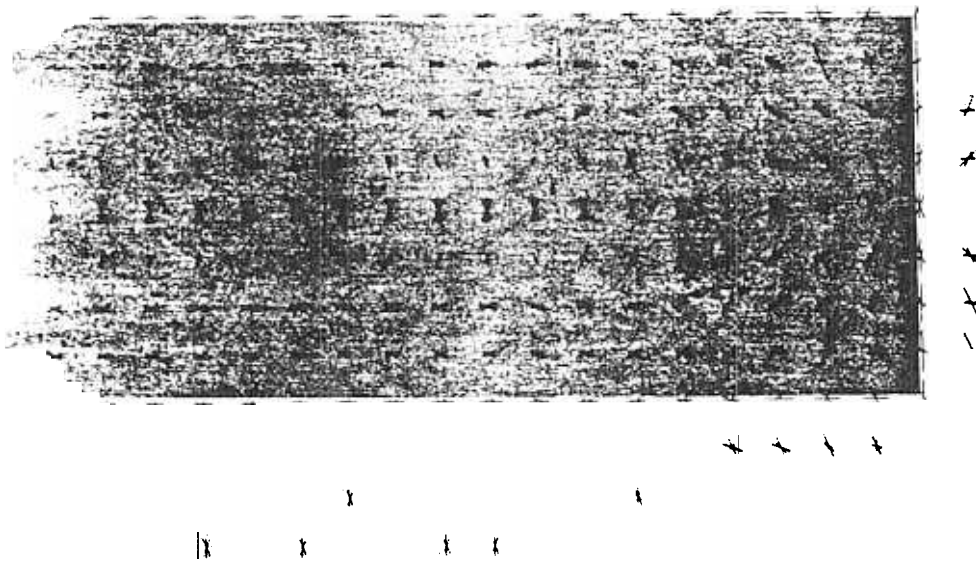
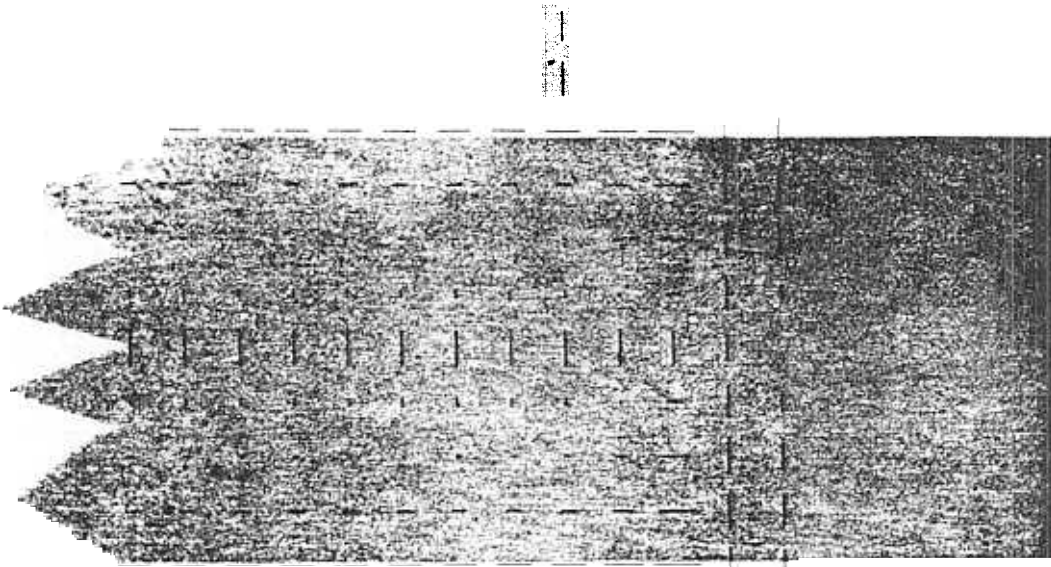OUTPUT OF ORIENTED MASKS

(b)

(a)

OUTPUT OF COMPETITION

(a)

(b)

with boundary contour signals within the monocular brightness and color stages MBC_L and MBC_R of Figure 4. and the manner in which these processing stages interact to generate a binocular percept at the BP stage of Figure 4. This analysis of brightness extends beyond the scope of this article. Cohen and Grossberg (in press) simulated a number of paradoxical brightness percepts that arise when observers inspect certain contoured images, such as the Craik–O'Brien effect (Arend et al., 1971; O'Brien, 1958) and its exceptions (Coren, 1983; Heggelund & Krekling, 1976; Todorović, 1983; Van den Brink & Keemink, 1976); the Bergström (1966, 1967a, 1967b) demonstrations comparing the brightnesses of smoothly modulated and steplike luminance profiles; Hamada's (1980) demonstrations of nonclassical differences between the perception of luminance decrements and increments; and Fechner's paradox, binocular brightness averaging, and binocular brightness summation (Blake, Sloane, & Fox, 1981; Cogan, 1982; Cogan, Silverman, & Sekuler, 1982; Curtis & Rule, 1980; Legge & Rubin, 1981; Levelt, 1965). Classical concepts such as spatial frequency analysis, Mach bands, and edge contrast are insufficient by themselves to explain the totality of these data. Because the monocular brightness domains do not know whether a boundary contour signal from the BCS stage is due to a "real" scenic contour or an "imaginary" scenic contour, these brightness simulations support our theory of boundary–feature interactions.

Cohen and Grossberg (1984) and Grossberg (1983a) showed through mathematical derivations and computer simulations how the binocular visual representations at the BP stage combine aspects of global depth, brightness, and form information. Grossberg (1980, 1983a, 1984a) used the theory to discuss the dynamics of monocular and binocular rivalry (Kaufman, 1974; Kulikowski, 1978; Rauschecker, Campbell, & Atkinson, 1973). Grossberg (1984a) indicated how the theory

can be used to explain fading of stabilized images (Yarbus, 1967).

Grossberg (1984a) also suggested how the theory can be extended to include color interactions. This extension provides a physical interpretation of the Land (1977) retinex theory. In this interpretation, a simultaneous parallel computation of contrast-sensitive feature contour signals occurs within double-opponent color processes (light–dark, red–green, yellow–blue). This parallel computation replaces Land's serial computation of edge contrasts along sampling paths that cross an entire visual scene. Despite Land's remarkable formal successes using this serial scanning procedure, it has not found a physical interpretation until the present time. One reason for this delay has been the absence of an explanation of why gradual changes in illumination between successive scenic contours are not perceived. The diffusive filling-in of feature contour signals within domains defined by boundary contour signals provides an explanation of this fundamental fact, as well as of Land's procedure of averaging the outcomes of many serial scans.

In addition to physically interpreting the Land retinex theory, the present theory also substantially generalizes the Land theory. The Land theory cannot, for example, explain any illusory brightness change that is due to the global configuration of the inducing elements, as in Figure 8a. The illusory circle in Figure 8a encloses a region of enhanced illusory brightness. No matter how many radially oriented serial scans of the Land theory are made between the radial lines, they will compute a total contrast change of zero, because there is no luminance difference between these lines. If one includes the black radial lines within the serial scans, then one still gets the wrong answer. This is seen by comparing Figure 8a and 8b. In these two figures, the number, length, contrast, and endpoints of the lines are the same. Yet Figure 8a generates a strong brightness dif-

---

Figure 23. (a) Response of the potentials y_{ijk} of a dipole field to the orientation field of Figure 22a. (End cutting generates horizontal activations at line and locations that receive small and orientationally ambiguous input activations. The oblique activations that occur at the line end can induce nonperpendicular illusory contours, as in Figure 9b.) (b) Response of the potentials y_{ijk} of a dipole field to the orientation field of Figure 22b. (End cutting generates "illusory" horizontal activations at the locations where vertically oriented inputs terminate.)

ference, whereas Figure 8b does not. This difference cannot be explained by any theory that depends only on averages of local contrast changes. The brightness effects are clearly due to the global configuration of the lines. A similar limitation of the Land theory is seen by comparing Figures 8 and 9, where rearranging the orientation of the line ends can alter the shape of the perceived region where enhanced brightness obtains.

Although the present theory physically interprets the Land retinex theory, it does not by any means provide a complete description of color processing by the nervous system. Much further work needs to be done, for example, to characterize how visual preprocessing generates color-specific, as opposed to merely wave-length sensitive, feature contour inputs into the featural filling-in syncytium (Zeki, 1983a, 1983b).

19. Related Data and Concepts About Illusory Contours

A variety of other workers have developed concepts based on their data that support our conception of boundary completion, although no one of them has explicitly posited the properties of the feature contour and boundary contour processes. Petry et al. (1983) wrote, for example, that "apparent brightness is influenced more by number of inducing elements, whereas apparent sharpness increases more with inducing element width . . . theoretical accounts of subjective contours must address both perceptual attributes" (p. 169), in support of our discussion in Sections 11 and 12. Day (1983) wrote that "illusory contours . . . are due primarily to the spread of induced contrast to partially delineated borders" (p. 488), in support of our concept of diffusive filling-in (Section 5), but he did not describe either how the borders are completed or how the featural induction and spread are accomplished. Prazdny (1983) studied variants of the illusion in Figure 8a. He concluded that "simultaneous brightness contrast is not a cause of the illusion" (p. 404) by replacing the black lines with alternating black and white rectangles on a gray background. In this way, he also demonstrated that illusory contours can be completed between scenic contours of opposite direction of contrast, as in Figure 2b, but he did not conclude from this that distinct boundary

contour and feature contour processes exist. Instead, he concluded that "It remains to be determined which of the competing 'cognitive' theories offers the best explanation . . . of subjective contours" (p. 404). Our results suggest that a cognitive theory is not necessary to explain the basic phenomena about subjective contours, unless one reinterprets *cognitive* to mean any network computation whose results are sensitive to the global patterning of all inducing elements.

20. Cortical Data and Predictions

Although the analysis that led to the boundary contour system and feature contour system was fueled by perceptual data, it has gradually become clear that a natural neural interpretation can be given to the processing stages of these systems. This linkage is suggested herein to predict unknown but testable neurophysiological properties, to provide a perceptual interpretation of known neural data, and to enable future data about visual cortex to more sharply constrain the development of perceptual theories.

We associate the early stages of left-monocular (MP_L) and right-monocular (MP_R) preprocessing in Figure 4 with the dynamics of the lateral geniculate nucleus, the first stages in the boundary contour system with the hypercolumns in striate cortex (Hubel & Wiesel, 1977), and the first stages in the feature contour system with the blobs in striate cortex (Hendrickson, Hunt, & Wu, 1981; Horton & Hubel, 1981). This interpretation is compatible with recent cortical data: The LGN projects directly to the hypercolumns as well as to the blobs (Livingstone & Hubel, 1982). The blobs are sensitive to color but not to orientation (Livingstone & Hubel, 1984), whereas the hypercolumns are sensitive to orientation but not to color (Hubel & Wiesel, 1977).

Given this neural labeling, the theory predicts that the blobs and the hypercolumns activate testably different types of cortical interactions. These interactions do not necessarily occur within the striate cortex, although they must be triggered by signals from the blobs and the hypercolumns.

The blobs are predicted to initiate featural filling-in. Hence, a single blob should be able to elicit a spreading effect among cells encoding the same featural quality (Figure 3). By

contrast, the hypercolumns are predicted to elicit boundary completion. Hence, pairs of similarly oriented and aligned hypercolumns must be activated before boundary completion over intervening boundary-sensitive cells can be activated (Figure 11). In other words, blobs are predicted to cause an *outwardly* directed featural spreading, whereas hypercolumns are predicted to cause an *inwardly* directed boundary completion.

Neural data that support our conception of how these interactions work are summarized below. Cells at an early stage in the boundary contour system are required to be sensitive to orientation and amount of contrast, but not to direction of contrast. Such *contour-sensitive cells* have been found in Area 17 of monkeys (Gouras & Krüger, 1979; Tanaka, Lee, & Creutzfeldt, 1983) as well as cats (Heggelund, 1981). These contour-sensitive cells are predicted to activate several stages of competition and cooperation that together contribute to the boundary completion process. The boundary completion process is predicted to be accomplished by a positive feedback exchange between cells reacting to long-range cooperation within an orientation and cells reacting to short-range competition between orientations (Figure 1). The competitive cells are predicted to occur at an earlier stage of cortical processing than the cooperative cells (Figure 18). These competitive cells are instrumental in generating a perpendicular end cut at the ends of lines (Figures 24 and 25). The cooperative cells are predicted to be segregated, possibly in distinct cortical lamina, according to the spatial range of their cooperative bandwidths (Figure 12).

The recent data of von der Heydt et al. (1984) support two of these predictions. These authors have reported the existence of cells in Area 18 of the visual cortex that help to "extrapolate lines to connect parts of the stimulus which might belong to the same object" (p. 1261). These investigators found these cells by using visual images that induce a percept of illusory figures in humans, as in Figures 2 and 8. Concerning the existence of a cooperative boundary completion process between similarly oriented and spatially aligned cells (Section 4), they write

Responses of cells in area 18 that required appropriately positioned and oriented luminance gradients when con-

ventional stimuli were used could often be evoked also by the corresponding illusory contour stimuli . . . The way widely separated picture elements contribute to a response resembles the function of logical gates." (pp. 1261–1262)

By *logical gates* they mean that two or more appropriately positioned and oriented scenic contours are needed to activate a response from an intervening cell, as in Figure 11. Concerning the existence of a competitive end-cutting process, they write "The responses to stimuli with lines perpendicular to the cell's preferred orientation reveal an unexpected new receptive field property" (p. 1262). The deep issue raised by these data can be expressed as follows. Why do cells that usually react to scenic edges parallel to their orientational preference also react to line ends that are perpendicular to their orientational preference? We provide an explanation of this property in Sections 11 and 13.

If we put these two types of experimental evidence together, the theory suggests that the contour-sensitive cells in Area 17 input to the cells that von der Heydt et al. (1984) have discovered in Area 18. A large number of physiological experiments can be designed to test this hypothesis, using stimuli such as those in Figure 2. For example, suppose that the contour-sensitive cells that would stimulate one end of the boundary completion process in response to a Kanizsa square are destroyed. Then the Area 18 cells that would normally be activated where the illusory boundary lies should remain silent. If these contour-sensitive cells could be reversibly inhibited, then the Area 18 cells should fire only when their triggering contour-sensitive cells in Area 17 are uninhibited. Informative experiments can also be done by selectively inhibiting boundary contour signals using stabilized image techniques. Suppose, for example, that the large circular boundary and the vertical boundary in Figure 24 are stabilized on the retina of a monkey. Then the cells that von der Heydt et al. discovered should stop firing at the corresponding Area 18 locations. This effect should also be reversible when image stabilization is terminated. The net impact of the experiments of von der Heydt et al. is thus to provide strong support for the concept of an inwardly directed boundary completion process and an orthogonally oriented end-
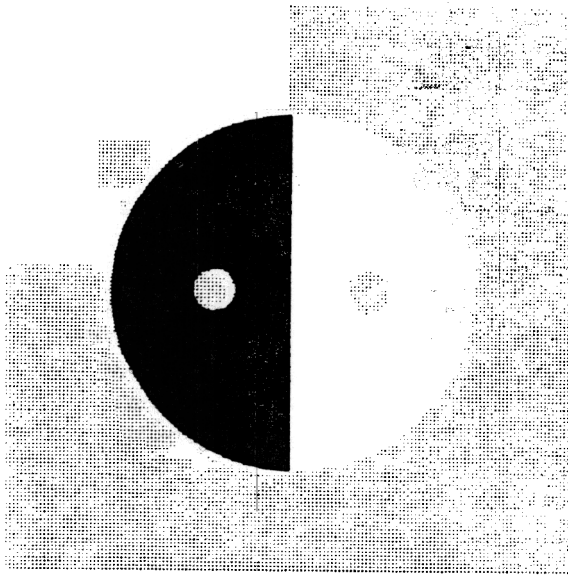
Figure 24. Contour stabilization leads to filling-in of color. (When the edges of the large circle and the vertical line are stabilized on the retina, the red color (dots) outside the large circle envelopes the black and white hemi-discs except within the small red circles whose edges are not stabilized (Yarbus, 1967). The red inside the left circle looks brighter and the red inside the right circle looks darker than the enveloping red.)

cutting process at the ends of lines, as well as a well-defined experimental methodology for testing finer aspects of these processes.

Concerning the *outwardly* directed featural filling-in process, a number of predictions can be made. The cellular syncytium that subserves the featural spreading is predicted to possess membranes whose ability to passively, or electrotonically, spread activation can be gated shut by boundary contour signals (Figure 3). The syncytium is hypothesized to be an evolutionary homolog of the intercellular interactions that occur among the retinal horizontal layers of certain fish (Usui, Mitarai, & Sakakibara, 1983). A possible cortical mechanism of this feature contour syncytium is some form of dendrodendritic coupling. Any manipulation that inhibits signals from the boundary contour system to the feature contour system (Pathways BCS — MBC_L and BCS — MBC_R of Figure 4) is predicted to release the syncytial flow, as well as to generate a percept of featural flow of colors and brightnesses. If *all* boundary contour signals are inhibited, so that no boundary restrictions of

featural flow occur, then a functional ganzfeld exists within the feature contour system. A dramatic reduction in visual sensitivity should occur, even if the feature contour system is otherwise intact.

An indirect behavioral test of how boundary contour signals restrict featural flow can be done using a stabilized image technique (Figure 24). Suppose that the large circular boundary and the vertical boundary in Figure 24 can be stabilized on the retina of a monkey. Train a monkey to press the first lever for food when it sees the unstabilized figure, and to press the second lever to escape shock when it sees a figure with a red background containing two small red circles of different shades of red, as in the stabilized percept. Then stabilize the relevant contours of Figure 24 and test which lever the monkey presses. If it presses the second lever with greater frequency than in the unstabilized condition, then one has behavioral evidence that the monkey perceives the stabilized image much as humans do. Also carry out electrode recordings of von der Heydt et al. (1984) cells at Area 18 locations corresponding to the stabilized image contours. If these cells stop firing during stabilization and if the monkey presses the second lever more at these times, then a featural flow that is contained by boundary contour signals is strongly indicated.

Figure 25 depicts a schematic top-down view of how boundary contour signals elicited by cortical hypercolumns could restrict the syncytial flow of featural quality elicited by cortical blobs. This flow does not necessarily occur among the blobs themselves. Figure 25 indicates, however, that the topographies of blobs and hypercolumns are well suited to serve as inputs to the cell syncytium. We suggest that the cell syncytium occurs somewhere between the blobs in Area 17 (also called *V1*) and the cells in Area V4 of the prestriate cortex (Zeki, 1983a, 1983b). The theory suggests that the cells of von der Heydt et al. (1984) project to the cell syncytium. Hence staining or electrophysiological techniques that reveal the projections of these cells may be used to locate the syncytium.

These experiments are illustrative rather than exhaustive of the many that are suggested by the theory.
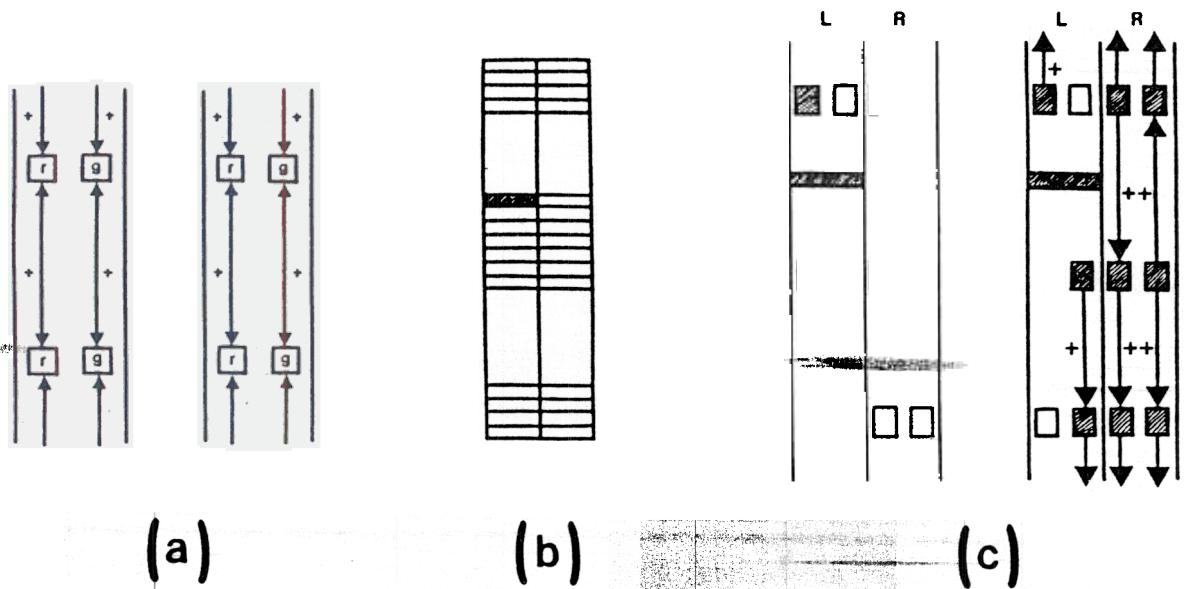
Figure 25. Predicted interactions due to signals from blobs and hypercolumns. ([a] In the absence of boundary contour signals, each blob can initiate featural spreading to blob-activated cells of like featural quality in a light–dark, red–green, blue–yellow double-opponent system. The symbols L and R signify signals initiated within left and right ocular dominance columns, respectively. The symbols r and g designate two different color systems; for example, the red and green double-opponent systems. The arrows indicate possible directions of featural filling-in. [b] An oriented boundary contour signal can be initiated from orientations at left-eye positions, right-eye positions, or both. The rectangular regions depict different orientationally tuned cells within a hypercolumn (Hubel & Wiesel, 1977). The shaded region is active. [c] These boundary contour signals are well positioned to attenuate the electrotonic flow of featural quality between contiguous perceptual positions. The shaded blob and hypercolumn regions are activated in the left figure. The arrows in the right figure illustrate how featural filling-in is restricted by the active boundary contour signal.)

21. Concluding Remarks

By articulating the boundary–feature trade-off, our theory shows that a sharp distinction between the boundary contour system and the feature contour system is needed to discover the rules that govern either system. Paradoxical percepts like neon color spreading can then be explained as consequences of adaptive mechanisms that prevent observers from perceiving a flow of featural quality from all line ends and corners due to orientational uncertainty. The theory's instantiation of featural filling-in, in turn, arises from an analysis of how the nervous system compensates for having discounted spurious illuminants, stabilized retinal veins, scotomas, and other imperfections of the retinal image. Once one accepts the fact that featural qualities can fill-in over discounted inputs, then the need for another contour system to restrict the featural flow seems inevitable.

A careful study of these contour systems reveals that they imply a strong statement about both the computational units and the types of visual representations that are used in other approaches to visual perception. We claim that local computations of scenic luminances, although useful for understanding some aspects of early visual processing, cannot provide an adequate understanding of visual perception because most scenic luminances are discounted as spurious by the human visual system. We also posit that physical processes of featural filling-in and boundary completion occur, as opposed to merely formal correspondences between external scenes and internal representations. Many contemporary contributors to perception eschew such physical approaches in order to avoid the pitfalls of naive realism. Despite the physical concreteness of the contour system processes, these processes do not support a philosophy of naive realism.

This can be seen most easily by considering how the activity patterns within the contour systems are related to the "conscious percepts" of the theory. For example, many perpendicular end cuts due to scenic line endings never reach consciousness in the theory. This property reflects the fact that the theory does not just rebuild the edges that exist "out there." Instead, the theory makes a radical break with classical notions of geometry by suggesting that a line is not even a collection of points. A line is, at least in part, the equilibrium set of a nonlinear cooperative–competitive dynamical feedback process. A line in the theory need not even form a connected set until it dynamically equilibrates, as Figures 20 and 21 demonstrate. This property may have perceptual significance, because a boundary contour cannot effectively restrict featural filling-in to become visible until it can separate two regions of different featural contrast. Initial surges of boundary completion may thus be competitively squelched before they reach consciousness, as in metacontrast phenomena.

In a similar vein, featural filling-in within a cell syncytium does not merely establish a point-to-point correspondence between the reflectances of a scene and corresponding positions within the cell syncytium. Until a boundary contour pattern is set up within the syncytium, the spatial domain within which featural contour inputs interact to influence prescribed syncytial cells is not even defined, let alone conscious.

Perhaps the strongest disclaimer to a naive realist viewpoint derives from the fact that *none* of the contour system interactions that have been discussed in this article are assumed to correspond to conscious percepts. All of these interactions are assumed to be preprocessing stages that may or may not lead to a conscious color-and-form-in-depth percept at the binocular percept stage of Figure 4. As during binocular rivalry (Kaufman, 1974; Kulikowski, 1978), a contoured scene that is easily perceived during monocular viewing is not always perceived when it is binocularly viewed along with a discordant scene to the other eye. A conscious percept is synthesized at the theory's BP stage using output signals from the two pairs of monocular contour

systems (Cohen & Grossberg, 1984, in press; Grossberg, 1983a). The formal cells within the BP stage are sensitive to spatial scale, orientation, binocular disparity, and the spatial distribution of featural quality. Many BP cells that receive inputs from the MBC_L and MBC_R stages are not active in the BP percept. Although the BP stage instantiates a physical process, this process represents an abstract context-sensitive representation of a scenic environment, not merely an environmental isomorphism. We believe that Area V4 of the prestriate cortex fulfills a similar function in vivo (Zeki, 1983a, 1983b).

Even when a conscious representation is established at the BP stage, the information that is represented in this way is quite limited. For example, the process of "seeing" a form at the BP stage does not imply that we can recognize the objects within that form. We hypothesize that the boundary contour system sends signals in parallel to the monocular brightness and color stages (MBC_L and MBC_R in Figure 4) as well as to an *object recognition system*. The top-down feedback from the object recognition system to the boundary contour system can provide "cognitive contour" signals that are capable of modulating the boundary completions that occur within the boundary contour system (Gregory, 1966; Grossberg, 1980, 1982, 1984b). Thus we envisage that two types of cooperative feedback—boundary completion signals and learned top-down expectancies—can monitor the synthesis of monocular boundary contours. For the same reasons that not all bottom-up activations of boundary contours become visible, not all top-down activations of boundary contours become visible. A boundary contour that is invisible at the BP stage can, however, have a strong effect on the object recognition system.

"Seeing" a BP form percept does not imply a knowledge of where an object is in space, any more than it implies a knowledge of which object is being seen. Nonetheless, just as the same network laws are being used to derive networks for color and form perception and for object recognition, so too are these laws being used to analyze how observers learn to generate accurate movements in response to visual cues (Grossberg, 1978, 1985,

in press; Grossberg & Kuperstein, 1985). This work on sensory–motor control suggests how a neural network as a whole can accurately learn to synthesize and calibrate sensory–motor transformations in real-time even though its individual cells cannot do so, and even if the cellular parameters from which these networks are built may be different across individuals, may change during development, and may be altered by partial injuries throughout life.

Our most sweeping reply to the criticism of naive realism is thus that a single set of dynamical laws can be used, albeit in specialized wiring diagrams, for the explanation of data that, on the level of naive experience, could not seem to be more different. Using such laws, the present theory promises to provide a significant synthesis of perceptual and neural data and theories. Spatial frequencies and oriented receptive fields are both necessary but not sufficient. The perceptual interpretation of the blobs and hypercolumns strengthens the arguments for parallel cortical processing, but the need for several stages of processing leading to a unitary percept also strengthens the arguments for hierarchical cortical processing. A role for propagated action potentials in the boundary contour system is balanced by a role for electrotonic processing in the feature contour system. Relatively local cortical processing is needed to compute receptive field properties, but relatively global cortical interactions are needed to generate unambiguous global percepts, such as those of perceptual boundaries, from ambiguous local cues.

The deepest conceptual issues raised by the present results concern the choice of perceptual units and neural design principles. The impoverished nature of the retinal image and a huge perceptual data base about visual illusions show that local computations of pointwise scenic luminances cannot provide an adequate understanding of visual perception. The boundary–feature trade-off suggests that the visual system is designed in a way that is quite different from any possible local computational theory. This insight promises to be as important for the design of future computer vision and robotics algorithms as

it may be for progress in perceptual and neural theory.

References

Arend, L. E., Buehler, J. N., & Lockhead, G. R. (1971). Difference information in brightness perception. *Perception and Psychophysics, 9,* 367–370.

Beck, J., Prazdny, K., & Rosenfeld, A. (1983). A theory of textural segmentation. In J. Beck, B. Hope, & A. Rosenfeld (Eds.), *Human and machine vision* (pp. 1–38). New York: Academic Press.

Bergström, S. S. (1966). A paradox in the perception of luminance gradients, 1. *Scandinavian Journal of Psychology, 7,* 209–224.

Bergström, S. S. (1967a). A paradox in the perception of luminance gradients, 2. *Scandinavian Journal of Psychology, 8,* 25–32.

Bergström, S. S. (1967b). A paradox in the perception of luminance gradients, 3. *Scandinavian Journal of Psychology, 8,* 33–37.

Biederman, I. (1984). Personal communication.

Blake, R., Sloane, M., & Fox, R. (1981). Further developments in binocular summation. *Perception and Psychophysics, 30,* 266–276.

Boynton, R. M. (1975). Color, hue, and wavelength. In E. C. Carterette & M. P. Friedman (Eds.), *Handbook of perception: Seeing* (Vol. 5, pp. 301–347). New York: Academic Press.

Carpenter, G. A., & Grossberg, S. (1981). Adaptation and transmitter gating in vertebrate photoreceptors. *Journal of Theoretical Neurobiology, 1,* 1–42.

Carpenter, G. A., & Grossberg, S. (1983). Dynamic models of neural systems: Propagated signals, photoreceptor transduction, and circadian rhythms. In J. P. E. Hodgson (Ed.), *Oscillations in mathematical biology* (pp. 102–196). New York: Springer-Verlag.

Cogan, A. L. (1982). Monocular sensitivity during binocular viewing. *Vision Research, 22,* 1–16.

Cogan, A. L., Silverman, G., & Sekuler, R. (1982). Binocular summation in detection of contrast flashes. *Perception and Psychophysics, 31,* 330–338.

Cohen, M. A., & Grossberg, S. (1983). Neural dynamics of binocular form perception. *Neuroscience Abstracts, 13,* No. 353.8.

Cohen, M. A., & Grossberg, S. (1984). Some global properties of binocular resonances: Disparity matching, filling-in, and figure-ground synthesis. In P. Dodwell & T. Caelli (Eds.), *Figural synthesis* (pp. 117–151). Hillsdale, NJ: Erlbaum.

Cohen, M. A., & Grossberg, S. (in press). Neural dynamics of brightness perception: Features, boundaries, diffusion, and resonance. *Perception and Psychophysics.*

Coren, S. (1983). When "filling-in" fails. *Behavioral and Brain Sciences, 6,* 661–662.

Cornsweet, T. N. (1970). *Visual perception.* New York: Academic Press.

Curtis, D. W., & Rule, S. J. (1980). Fechner's paradox reflects a nonmonotone relation between binocular brightness and luminance. *Perception and Psychophysics, 27,* 263–266.

Day, R. H. (1983). Neon color spreading, partially delin-

eated borders. and the formation of illusory contours. *Perception and Psychophysics, 34*, 488–490.

DeValois. R. L.. & DeValois, K. K. (1975). Neural coding of color. In E. C. Carterette & M. P. Friedman (Eds.), *Handbook of perception: Seeing* (Vol. 5, pp. 117–166). New York: Academic Press.

Gellatly, A. R. H. (1980). Perception of an illusory triangle with masked inducing figure. *Perception, 9*, 599–602.

Gerrits, H. J. M., de Haan, B., & Vendrick, A. J. H. (1966). Experiments with retinal stabilized images: Relations between the observations and neural data. *Vision Research, 6*, 427–440.

Gerrits, H. J. M., & Timmerman, J. G. M. E. N. (1969). The filling-in process in patients with retinal scotomata. *Vision Research, 9*, 439–442.

Gerrits, H. J. M., & Vendrick, A. J. H. (1970). Simultaneous contrast, filling-in process and information processing in man's visual system. *Experimental Brain Research, 11*, 411–430.

Glass, L., & Switkes, E. (1976). Pattern recognition in humans: Correlations which cannot be perceived. *Perception, 5*, 67–72.

Gouras, P., & Krüger, J. (1979). Responses of cells in foveal visual cortex of the monkey to pure color contrast. *Journal of Neurophysiology, 42*, 850–860.

Graham, N. (1981). The visual system does a crude Fourier analysis of patterns. In S. Grossberg (Ed.), *Mathematical psychology and psychophysiology* (pp. 1–16). Providence, RI: American Mathematical Society.

Graham, N., & Nachmias, J. (1971). Detection of grating patterns containing two spatial frequencies: A test of single-channel and multiple-channel models. *Vision Research, 11*, 251–259.

Gregory, R. L. (1966). *Eye and brain.* New York: McGraw-Hill.

Grossberg, S. (1973). Contour enhancement, short term memory, and constancies in reverberating neural networks. *Studies in Applied Mathematics, 52*, 217–257.

Grossberg, S. (1976). Adaptive pattern classification and universal recoding, II: Feedback, expectation, olfaction, and illusions. *Biological Cybernetics, 23*, 187–202.

Grossberg, S. (1978). A theory of human memory: Self-organization and performance of sensory–motor codes, maps, and plans. In R. Rosen & F. Snell (Eds.), *Progress in theoretical biology* (Vol. 5, pp. 233–374). New York: Academic Press.

Grossberg, S. (1980). How does a brain build a cognitive code? *Psychological Review, 87*, 1–51.

Grossberg, S. (1981). Adaptive resonance in development, perception, and cognition. In S. Grossberg (Ed.), *Mathematical psychology and psychophysiology* (pp. 107–156). Providence, RI: American Mathematical Society.

Grossberg, S. (1982). *Studies of mind and brain: Neural principles of learning, perception, development, cognition, and motor control.* Boston: Reidel Press.

Grossberg, S. (1983a). The quantized geometry of visual space: The coherent computation of depth, form, and lightness. *Behavioral and Brain Sciences, 6*, 625–692.

Grossberg, S. (1983b). Neural substrates of binocular form perception: Filtering, matching, diffusion, and resonance. In E. Basar, H. Flohr, H. Haken & A. J. Mandell (Eds.), *Synergetics of the brain* (pp. 274–298). New York: Springer-Verlag.

Grossberg, S. (1984a). Outline of a theory of brightness, color, and form perception. In E. DeGreef & J. van Buggenhaut (Eds.), *Trends in mathematical psychology* (pp. 59–86). Amsterdam: North-Holland.

Grossberg, S. (1984b). Some psychophysiological and pharmacological correlates of a developmental, cognitive, and motivational theory. In R. Karrer, J. Cohen, & P. Tueting (Eds.), *Brain and information: Event related potentials* (pp. 58–151). New York: New York Academy of Sciences.

Grossberg, S. (1985). The adaptive self-organization of serial order in behavior: Speech, language, and motor contol. In E. C. Schwab & H. C. Nusbaum (Eds.), *Perception of speech and visual form: Theoretical issues, models, and research.* New York: Academic Press.

Grossberg, S. (in press). The role of learning in sensory–motor control. *Behavioral and Brain Sciences.*

Grossberg, S., & Cohen, M. A. (1984). Dynamics of brightness and contour perception. Supplement to *Investigative Ophthalmology and Visual Science, 25*, 71.

Grossberg, S., & Kuperstein, M. (1985). *Neural dynamics of adaptive sensory–motor control: Ballistic eye movements.* Amsterdam: North-Holland.

Grossberg, S., & Mingolla, E. (1984). The neural dynamics of perceptual grouping: Textures, borders, and incomplete figural contours. Manuscript submitted for publication.

Hamada, J. (1980, July). Antagonistic and non-antagonistic processes in the lightness perception. *Proceedings of the XXII International Congress of Psychology,* Leipzig, E. Germany.

Heggelund, P. (1981). Receptive field organization of complex cells in cat striate cortex. *Experimental Brain Research, 42*, 99–107.

Heggelund, P., & Krekling, S. (1976). Edge dependent lightness distributions at different adaptative levels. *Vision Research, 16*, 493–496.

Helmholtz, H. von (1962). *Physiological optics* (J. P. C. Southall, Trans.). New York: Dover.

Hendrickson, A. E., Hunt, S. P., & Wu, J.-Y. (1981). Immunocytochemical localization of glutamic acid decarboxylase in monkey striate cortex. *Nature, 292*, 605–607.

Horton, J. C., & Hubel, D. H. (1981). Regular patchy distribution of cytochrome oxidase staining in primary visual cortex of macaque monkeys. *Nature, 292*, 762–764.

Hubel, D. H., & Livingstone, M. S. (1981). Regions of poor orientation tuning coincide with patches of cytochrome oxidase staining in monkey striate cortex. *Neuroscience Abstracts, 11*, No. 118.12.

Hubel, D. H., & Wiesel, T. N. (1977). Functional architecture of macaque monkey visual cortex. *Proceedings of the Royal Society of London (B), 198*, 1–59.

Julesz, B. (1971). *Foundations of cyclopean perception.* Chicago: University of Chicago Press.

Kanizsa, G. (1974). Contours without gradients or cognitive contours? *Italian Journal of Psychology, 1*, 93–113.

Kanizsa, G. (1976). Subjective contours. *Scientific American, 234*, pp. 48–64.

Kaufman, L. (1974). *Sight and mind: An introduction to visual perception.* New York: Oxford University Press.

Kennedy, J. M. (1978). Illusory contours and the ends of lines. *Perception, 7,* 605–607.

Kennedy, J. M. (1979). Subjective contours, contrast, and assimilation. In C. F. Nodine & D. F. Fisher (Eds.), *Perception and pictorial representation* (pp. 167–195). New York: Praeger.

Kennedy, J. M. (1981). Illusory brightness and the ends of petals: Change in brightness without aid of stratification or assimilation effects. *Perception, 10,* 583–585.

Kennedy, J. M., & Ware, C. (1978). Illusory contours can arise in dot figures. *Perception, 7,* 191–194.

Krauskopf, J. (1963). Effect of retinal image stabilization on the appearance of heterochromatic targets. *Journal of the Optical Society of America, 53,* 741–744.

Kulikowski, J. J. (1978). Limit of single vision in stereopsis depends on contour sharpness. *Nature, 275,* 126–127.

Land, E. H. (1977). The retinex theory of color vision. *Scientific American, 237,* 108–128.

Leeper, R. (1935). A study of a neglected portion of the field of learning—the development of sensory organization. *Journal of Genetic Psychology, 46,* 41–75.

Legge, G. E., & Rubin, G. S. (1981). Binocular interactions in suprathreshold contrast perception. *Perception and Psychophysics, 30,* 49–61.

Levelt, W. J. M. (1965). *On binocular rivalry.* Soesterberg, The Netherlands: Institute for Perception, RVO-TNO.

Livingstone, M. S., & Hubel, D. H. (1982). Thalamic inputs to cytochrome oxidase-rich regions in monkey visual cortex. *Proceedings of the National Academy of Sciences, 79,* 6,098–6,101.

Livingstone, M. S., & Hubel, D. H. (1984). Anatomy and physiology of a color system in the primate visual cortex. *Journal of Neuroscience, 4,* 309–356.

Mingolla, E., & Grossberg, S. (1984). Dynamics of contour completion: Illusory figures and neon color spreading. Supplement to *Investigative Ophthalmology and Visual Science, 25,* 71.

Mollon, J. D., & Sharpe, L. T. (Eds.) (1983). *Colour vision.* New York: Academic Press.

O'Brien, V. (1958). Contour perception, illusion, and reality. *Journal of the Optical Society of America, 48,* 112–119.

Parks, T. E. (1980). Subjective figures: Some unusual concomitant brightness effects. *Perception, 9,* 239–241.

Parks, T. E., & Marks, W. (1983). Sharp-edged vs. diffuse illusory circles: The effects of varying luminance. *Perception and Psychophysics, 33,* 172–176.

Petry, S., Harbeck, A., Conway, J., & Levey, J. (1983). Stimulus determinants of brightness and distinctness of subjective contours. *Perception and Psychophysics, 34,* 169–174.

Prazdny, K. (1983). Illusory contours are not caused by simultaneous brightness contrast. *Perception and Psychophysics, 34,* 403–404.

Pritchard, R. M. (1961). Stabilized images on the retina. *Scientific American, 204,* 72–78.

Pritchard, R. M., Heron, W., & Hebb, D. O. (1960). Visual perception approached by the method of stabilized images. *Canadian Journal of Psychology, 14,* 67–77.

Rauschecker, J. P. J., Campbell, F. W., & Atkinson, J. (1973). Colour opponent neurones in the human visual system. *Nature, 245,* 42–45.

Redies, C., & Spillmann, L. (1981). The neon color effect in the Ehrenstein illusion. *Perception, 10,* 667–681.

Riggs, L. A., Ratliff, F., Cornsweet, J. C., & Cornsweet, T. N. (1953). The disappearance of steadily fixated visual test objects. *Journal of the Optical Society of America, 43,* 495–501.

Tanaka, M., Lee, B. B., & Creutzfeldt, O. D. (1983). Spectral tuning and contour representation in area 17 of the awake monkey. In J. D. Mollon & L. T. Sharpe (Eds.), *Colour vision* (pp. 269–276). New York: Academic Press.

Todorović, D. (1983). *Brightness perception and the Craik-O'Brien-Cornsweet effect.* Unpublished master's thesis, University of Connecticut, Storrs.

Usui, S., Mitarai, G., & Sakakibara, M. (1983). Discrete nonlinear reduction model for horizontal cell response in the carp retina. *Vision Research, 23,* 413–420.

Van den Brink, G., & Keemink, C. J. (1976). Luminance gradients and edge effects. *Vision Research, 16,* 155–159.

Van Tuijl, H. F. J. M. (1975). A new visual illusion: Neonlike color spreading and complementary color induction between subjective contours. *Acta Psychologica, 39,* 441–445.

Van Tuijl, H. F. J. M., & de Weert, C. M. M. (1979). Sensory conditions for the occurrence of the neon spreading illusion. *Perception, 8,* 211–215.

Van Tuijl, H. F. J. M., & Leeuwenberg, E. L. J. (1979). Neon color spreading and structural information measures. *Perception and Psychophysics, 25,* 269–284.

von der Heydt, R., Peterhans, E., & Baumgartner, G. (1984). Illusory contours and cortical neuron responses. *Science, 224,* 1260–1262.

Ware, C. (1980). Coloured illusory triangles due to assimilation. *Perception, 9,* 103–107.

Yarbus, A. L. (1967). *Eye movements and vision.* New York: Plenum Press.

Zeki, S. (1983a). Colour coding in the cerebral cortex: The reaction of cells in monkey visual cortex to wavelengths and colours. *Neuroscience, 9,* 741–765.

Zeki, S. (1983b). Colour coding in the cerebral cortex: The responses of wavelength-selective and colour coded cells in monkey visual cortex to changes in wavelength composition. *Neuroscience, 9,* 767–791.

(Appendix follows on next page)

Appendix

Dynamics of Boundary Formation

A network that instantiates the qualitative requirements described in the text will now be defined in stages, so that the basic properties of each stage can be easily understood. At each stage, we chose the simplest instantiation of the computational idea.

Oriented Masks

To define a mask centered at Position (i, j) with orientation k, divide the rectangular receptive field of the mask into a left-rectangle L_{ijk} and a right-rectangle R_{ijk}. Suppose that all the masks sample a field of preprocessed inputs. Let S_{pq} equal the preprocessed input to the position (p, q) of this field. The output J_{ijk} from the mask at Position (i, j) with orientation k is then defined by

$$J_{ijk} = \frac{[U_{ijk} - \alpha V_{ijk}]^+ + [V_{ijk} - \alpha U_{ijk}]^+}{1 + \beta(U_{ijk} + V_{ijk})}, \quad (A1)$$

where

$$U_{ijk} = \sum_{(p,q)\in L_{ijk}} S_{pq}, \quad (A2)$$

$$V_{ijk} = \sum_{(p,q)\in R_{ijk}} S_{pq}, \quad (A3)$$

and the notation $[p]^+ = \max(p, 0)$. In (A1), term

$$[U_{ijk} - \alpha V_{ijk}]^+ > 0 \quad (A4)$$

only if $U_{ijk}/V_{ijk} > \alpha$. Because U_{ijk} measures the total input to the left rectangle L_{ijk} and V_{ijk} measures the total input to the right rectangle R_{ijk}, inequality (A4) says that the input to L_{ijk} exceeds that to R_{ijk} by the factor α. Parameter $\alpha(\geq 1)$ thus measures the relative contrast between the left and right halves of the receptive field. The sum of two terms in the numerator of (A1) says that J_{ijk} is sensitive to the amount of contrast, but not to the direction of contrast, received by L_{ijk} and R_{ijk}. The denominator term in (A1) enables J_{ijk} to compute a ratio scale in the limit where $\beta(U_{ijk} + V_{ijk})$ is much greater than 1.

Intraorientational Competition Between Positions

As in Figure 18, inputs J_{ijk} with a fixed orientation k activate potentials w_{ijk} with the same orientation via on-center off-surround interactions. To achieve a disinhibitory capability, all potentials w_{ijk} are also excited by the same tonically active input I. Suppose that the excitatory inputs are not large enough to saturate their potentials, but that the inhibitory inputs can shunt their potentials toward small values. Then

$$\frac{d}{dt} w_{ijk} = -w_{ijk} + \ + f(J_{ijk})$$
$$- w_{ijk} \sum_{(p,q)} f(J_{pqk})D_{pqij}, \quad (A5)$$

where D_{pqij} is the inhibitory interaction strength between Positions (p, q) and (i, j), and $f(J_{ijk})$ is the input signal generated by J_{ijk}. Suppose, for simplicity, that

$$f(J_{ijk}) = \gamma J_{ijk}, \quad (A6)$$

where γ is a positive constant. Also suppose that w_{ijk} equilibrates rapidly to its inputs through time and is thus always approximately at equilibrium. Setting $\frac{d}{dt} w_{ijk} = 0$ in (A5), we find that

$$w_{ijk} = \frac{I + \gamma J_{ijk}}{1 + \gamma \sum_{(p,q)} J_{pqk}D_{pqij}} \quad (A7)$$

Dipole Competition Between Perpendicular Orientations

Perpendicular potentials w_{ijk} and w_{ijK} elicit output signals that compete at their target potentials x_{ijk} and x_{ijK}, respectively (Figure 18). Assume that these output signals equal the potentials of w_{ijk} and w_{ijK}, which are always nonnegative by (A7), and that x_{ijk} and x_{ijK} respond quickly to these signals within their linear dynamical range. Then

$$x_{ijk} = w_{ijk} - w_{ijK} \quad (A8)$$

and

$$x_{ijK} = w_{ijK} - w_{ijk}$$

Output signals are, in turn, generated by x_{ijk} and x_{ijK} when they exceed a nonnegative threshold. Let this threshold equal zero and suppose that the output signals $O_{ijk} = O(x_{ijk})$ and $O_{ijK} = O(x_{ijK})$ grow linearly above threshold. Then

$$O_{ijk} = C[w_{ijk} - w_{ijK}]^+ \quad (A10)$$

and

$$O_{ijK} = C[w_{ijK} - w_{ijk}]^+, \quad (A11)$$

where C is a positive constant and $[p]^+ = \max(p, 0)$.

Interorientational Competition Within a Position

Let the outputs O_{ijk}, $k = 1, 2, \ldots, n$, be the inputs to an orientationally tuned on-center off-surround competition within each position. The potential y_{ijk} is excited by O_{ijk} and inhibited by all

O_{ijm}, m $\neq$ k. Potential y_{ijk} therefore obeys the shunting on-center off-surround equation (Grossberg, 1983a)

$$\frac{d}{dt} y_{ijk} = -Ay_{ijk} + (B - y_{ijk})O_{ijk}$$

$$- y_{ijk} \sum_{m \neq k} O_{ijm} \quad (A12)$$

Suppose that y_{ijk} also equilibrates rapidly to its inputs. Setting $\frac{d}{dt} y_{ijk} = 0$ in (A12) implies that

$$y_{ijk} = \frac{BO_{ijk}}{A + O_{ij}}, \quad (A13)$$

where

$$O_{ij} = \sum_{m=1}^{n} O_{ijm}. \quad (A14)$$

By equation (A13), the total activity

$$y_{ij} = \sum_{m=1}^{n} y_{ijm} \quad (A15)$$

tends to be conserved because

$$y_{ij} = \frac{BO_{ij}}{A + O_{ij}}. \quad (A16)$$

Thus if A is small compared to O_{ij}, then $y_{ij} \cong B$.

Oriented Cooperation

As in Figure 19, if two (sets of) output signals $f(y_{ijk})$ and $f(y_{uvk})$ can trigger supraliminal activation of an intervening boundary completion potential z_{pqk}, then positive feedback from z_{pqk} to x_{pqk} can initiate a rapid completion of a boundary with orientation k between Positions (i, j) and (u, v). The following equation illustrates a rule for activating a boundary completion potential z_{ijk} due to properly aligned pairs of outputs:

$$\frac{d}{dt} z_{ijk} = -z_{ijk} + g(\sum_{(p,q)} f(y_{pqk})E_{pqij}^{(k)})$$

$$+ g(\sum_{(p,q)} f(y_{pqk})F_{pqij}^{(k)}). \quad (A17)$$

In (A17), $g(s)$ is a signal function that becomes positive only when s is positive, and has a finite maximum value. A sum of two sufficiently positive $g(s)$ terms in (A17) is needed to activate z_{ijk} above the firing threshold of its output signal $h(z_{ijk})$. The output signal function $h(s)$ is chosen faster-than-linear, and with a large slope to help choose orientation k in position (i, j). Each sum

$$\sum_{(p,q)} f(y_{pqk})E_{pqij}^{(k)}$$

and

$$\sum_{(p,q)} f(y_{pqk})F_{pqij}^{(k)}$$

adds up outputs from a strip with orientation k that lies to one side or the other of Position (i, j), as in Figure 11. The oriented kernels $E_{pqij}^{(k)}$ and $F_{pqij}^{(k)}$ accomplish this process of anisotropic averaging. A set of modestly large $f(y_{pqk})$ outputs within the bandwidth of $E_{pqij}^{(k)}$ or $F_{pqij}^{(k)}$ can thus have as much of an effect on z_{ijk} as a single larger $f(y_{pqk})$ output. This property contributes to the statistical nature of the boundary completion process. An equation in which the sum of $g(w)$ terms in (A17) is replaced by a product of $g(w)$ terms works just as well formally. At equilibrium, (A17) implies that

$$z_{ijk} = g(\sum_{(p,q)} f(y_{pqk})E_{pqij}^{(k)})$$

$$+ g(\sum_{(p,q)} f(y_{pqk})F_{pqij}^{(k)}). \quad (A18)$$

The effect of boundary completion feedback signals $h(z_{ijk})$ on the (i, j) position is described by changing the equation (A7) to

$$w_{ijk} = \frac{I + \gamma J_{ijk} + h(z_{ijk})}{1 + \gamma \sum_{(p,q)} J_{pqk}D_{pqij}}. \quad (A19)$$

Equations (A1), (A19), (A10), (A13), and (A18), respectively, define the equilibrium of the network, up to parameter choices. This system is summarized below for completeness.

$$J_{ijk} = \frac{[U_{ijk} - \alpha V_{ijk}]^+ + [V_{ijk} - \alpha U_{ijk}]^+}{1 + \beta(U_{ijk} + V_{ijk})},$$

$$w_{ijk} = \frac{I + \gamma J_{ijk} + h(z_{ijk})}{1 + \gamma \sum_{(p,q)} J_{pqk}D_{pqij}},$$

$$O_{ijk} = C[w_{ijk} - w_{ijK}]^+,$$

$$y_{ijk} = \frac{BO_{ijk}}{A + O_{ij}},$$

and

$$z_{ijk} = g(\sum_{(p,q)} f(y_{pqk})E_{pqij}^{(k)}) + g(\sum_{(p,q)} f(y_{pqk})F_{pqij}^{(k)}).$$

Although these equilibrium equations compactly summarize the computational logic of competitive-cooperative boundary contour interactions, a full understanding of the information processing capabilities of this network requires a study of the corresponding differential equations, not just their equilibrium values. The equations for feature contour signals and diffusive filling-in are described in Cohen and Grossberg (in press).